Higgs mass from neutrino-messenger mixing

Pritibhajan Byakti,[a,b] **Charanjit K Khosa,**[a] **V. S. Mummidi,**[c] **Sudhir K Vempati**[a]

[a] *Center for High Energy Physics,*
Indian Institute of Science, Bangalore 560012, INDIA
[b] *Department of Theoretical Physics,*
Indian Association for the Cultivation of Science,
2A & 2B Raja S.C. Mullick Road, Kolkata 700 032, INDIA
[c] *Harish-Chandra Research Institute,*
Chhatnag Road, Jhusi, Allahabad 211019, INDIA

E-mail: tppb@iacs.res.in, khosacharanjit@chep.iisc.ernet.in,
venkatasuryanarayana@hri.res.in, vempati@chep.iisc.ernet.in

arXiv:1607.03447v2 [hep-ph] 16 Mar 2017

Abstract: The discovery of the Higgs particle at 125 GeV has put strong constraints on minimal messenger models of gauge mediation, pushing the stop masses into the multi-TeV regime. Extensions of these models with matter-messenger mixing terms have been proposed to generate a large trilinear parameter, A_t, relaxing these constraints. The detailed survey of these models [1, 2] so far considered messenger mixings with only MSSM superfields. In the present work, we extend the survey to MSSM with inverse-seesaw mechanism. The neutrino-sneutrino corrections to the Higgs mass in the inverse seesaw model are not significant in the minimal gauge mediation model, unless one considers messenger-matter interaction terms. We classify all possible models with messenger-matter interactions and perform thorough numerical analysis to find out the promising models. We found that out of the 17 possible models 9 of them can lead to Higgs mass within the observed value without raising the sfermion masses significantly. The successful models have stop masses $\sim$1.5 TeV with small or negligible mixing and yet a light CP even Higgs at 125 GeV.

Contents

1 Introduction **1**

2 Recap of GMSB with and without matter-messenger mixing terms **3**
2.1 Matter-Messenger Interactions 4

3 Messenger-matter interactions involving leptons and neutrinos **6**
3.1 Inverse seesaw model 6
3.2 Classification of the models 9

4 Analysis of the models **11**
4.1 Model 1 12
4.2 Model 2 15
4.3 Model 3 16
4.4 Model 4 18
4.5 Model 5 21
4.6 Model 6 23
4.7 Model 7 24
4.8 Model 8 26
4.9 Model 9 28
4.10 Model 10 30
4.11 Model 11 31
4.12 Model 12 33
4.13 Model 13 36
4.14 Model 14 37
4.15 Model 15 41
4.16 Model 16 41
4.17 Model 17 44

5 Discussion and conclusions **45**

A One loop neutrino-sneutrino corrections to the Higgs mass **48**

1 Introduction

Supersymmetry (SUSY) [3–7] offers one of the most elegant solutions to the hierarchy problem. In the Minimal Supersymmetric Standard Model (MSSM) [7–9], the Higgs mass is protected from the dangerous UV sensitive radiative corrections. However, for various reasons, supersymmetry breaking cannot be incorporated in the MSSM in a straightforward

way. SUSY is spontaneously broken in a remote sector and the information is then passed to the MSSM sector through mediators. Among the different types of mediation mechanisms, gauge mediation (GMSB in short, for a review see [10]) is interesting as it generates soft parameters which are flavor diagonal.

The discovery of ∼125 GeV CP even neutral Higgs boson[11, 12] has however imposed strong constraints on GMSB models. To accommodate the light CP-even Higgs boson of that mass range, the spectrum of GMSB models had to become heavy [13]. Such a heavy spectrum is not 'natural' as it leads to larger fine tuning. Secondly, there is a bleak chance to discover any such particle at Large Hadron Collider (LHC). This is true for all the GMSB models which are characterized by small A-terms, including the most general one of general gauge mediation (GGM) [14, 15].

Several solutions have been put forward to remedy this situation. They can mainly be divided into two classes : (a) models which generate large A-terms through some mechanism[1, 2, 16–31] (b) models which augment to the Higgs mass through additional contributions while keeping the A-terms small. The former class is dominated by models which contain new interactions between messenger and matter fields. These generate the required A-terms for the stop sector, though some of them could suffer from other problems like A_t/m^2 problem [19]. In the second category several strategies are proposed, for example, $U(1)$ gauge group extension[32], NMSSM and/or vector matter [19, 33–46], SO(10) D terms [47] to name a few. Another way is to have an additional source of supersymmetry breaking, preferably mediated by gravitational interactions, such that it dominantly generates A_t and other related soft terms[48].

In the present work we will focus on the first class of models with messenger-matter interactions. A classification of all such models has been presented in Refs. [1, 2]) for MSSM. The classification in [2] concentrated on the messenger interactions with hadronic matter fields Q, U^c and the Higgs field H_u which are relevant for the A_t and other trilinear parameters. In Ref.[1], messenger and matter fields interact SU(5) multiplet-wise. As a consequence other fields like D^c, L, E^c and H_d also interact with the messengers in the studied models. In MSSM, the messenger matter interactions involving leptonic fields will not play any role in the generation of A_t or on the Higgs mass. However, the situation changes in the presence of an 'inverse' seesaw mechanism [49].

The standard seesaw mechanism with right handed neutrinos can have large Yukawa couplings $\sim \mathcal{O}(y_t)$, the corrections to the Higgs mass are tiny as the right handed neutrinos are very heavy, close to the GUT scale to give the correct neutrino masses (see Ref. [50] and references there in). On the other hand, inverse seesaw mechanism has additional singlets by which the right handed neutrino masses need not be very heavy and this enables corrections to the Higgs mass [49, 51, 52] which can be significant in some regions of the parameter space. There is however a caveat: the neutrino-sneutrino radiative corrections to the Higgs mass are different compared to the top-stop corrections. In the limit of large right handed neutrino masses, $m_R \gg m_{\tilde{\nu}}$ the neutrino and the sneutrino corrections to the Higgs mass cancel each other leading to negligible enhancement to the Higgs mass[51, 52]. However, there are two situations when the corrections to the Higgs mass can be significant: (a) if the slepton and sneutrino masses are comparable to $\sim m_R$, typically in

the multi-TeV regime and (b) the trilinear parameter associated with the neutrino Yukawa, X_N is large, leading to large mixing in the sneutrino sector. For case: (a) large slepton masses are not natural in minimal versions of GMSB. One possibility is to consider GGM boundary conditions with a separate and large slepton masses as boundary conditions[52]. For case:(b), trilinear parameters are generally small in minimal messenger models of gauge mediation. To generate large trilinear sneutrino mixing parameter, we consider matter-messenger mixing in the present paper.

As mentioned earlier, we extended the classification of the messenger-matter interaction models to the lepton and neutrino fields. We found that there are 17 models which are tabulated in Table 1. Considering GMSB boundary conditions along with these neutrino-messenger couplings we show that light stops can give Higgs mass $\sim$ 125 GeV in nine of these models. In these mixing models, only the third generation is allowed to couple with messengers. Hence we are safe from flavor constraints.

The paper organizes as follows. In § 2 we summarize gauge mediated SUSY breaking with and without mixing. Then we discuss inability of inverse seesaw models to produce correct Higgs mass in § 3 and motivate the study of messenger-matter interaction involving leptons and right handed neutrino fields. We classify the models based on the messenger-matter interactions. In § 4 classified models are analyzed in detail. Finally in § 5 we conclude.

2 Recap of GMSB with and without matter-messenger mixing terms

Gauge mediated SUSY breaking models consist of three sectors: (a) visible sector, (b) messenger sector, and (c) hidden sector. We do not know much about the hidden sector. However it is assumed that SUSY is spontaneously broken there and information of SUSY breaking is encoded in the spurion field X. Vacuum expectation value (VEV) of this spurion field is: $\langle X\rangle = M + \theta^2 F$ where M is the messenger scale and F is SUSY breaking VEV. The spurion field has superpotential level interaction with the messenger fields Φ_m as follows:

$$W_{\rm mes} = f X \sum_i \bar{\Phi}_{im}\Phi_{im}, \tag{2.1}$$

where superfield $\bar{\Phi}_m$ is conjugate representation of Φ_m under SM gauge group. In principle one can have complicated version of the above model; however, it is the simplest one and is called minimal GMSB (mGMSB) model. In general, messenger fields are multiplets of SU(5) like 5, 10 and 15 dimensional representations. Messenger fields are not, in general, considered to be incomplete multiplets of SU(5) as it may destroy one of beautiful features of MSSM, which is the unification of gauge coupling constants. However one can use incomplete multiplets as messengers without spoiling unification in special cases [53, 54].

Because of non-zero F-term VEV of X, messenger sector is not supersymmetric. As the messenger fields are charged under gauge groups, the SUSY breaking information passes to the visible sector through gauge interactions. Gaugino masses are generated at 1-loop level:

$$M_r = \frac{\alpha_r}{4\pi} d\, N\, \Lambda\, g(x), \tag{2.2}$$

where $r = 1, 2, 3$ represents U(1), SU(2) and SU(3) groups respectively, $\alpha_r = g_r^2/4\pi$, $\Lambda = F/M$, $x = F/M^2$, d is the Dynkin index, N is the number of messengers and the function $g(x)$ has the following form:

$$g(x) = \frac{1}{x^2}\left[(1+x)\ln(1+x)\right] + (x \to -x)\,. \tag{2.3}$$

Scalar soft mass squares are generated at 2-loop level,

$$M^2_{\tilde{a}\,\text{usual}} = 2N\,d\,\Lambda^2\left[\sum_r C_r(a)\left(\frac{\alpha_r}{4\pi}\right)^2\right] f(x), \tag{2.4}$$

where $C_r(a)$ is the quadratic Casimir of the representation of the MSSM field labeled by 'a' and the group corresponding to r , $\tilde{a}$ is the super-partner of the field a, and the function $f(x)$ has the following form:

$$f(x) = \frac{1+x}{x^2}\left[\ln(1+x) - 2Li_2\left(\frac{x}{1+x}\right) + \frac{1}{2}Li_2\left(\frac{2x}{1+x}\right)\right] + (x \to -x)\,. \tag{2.5}$$

Note that gaugino masses are proportional to N whereas the sfermion masses are proportional to $\sqrt{N}$. Thus one can have heavier gauginos with fixed sfermion masses for a larger N. Same is also true for the Dynkin index d. One gets heavier gauginos with fixed sfermion masses for a $10 \oplus \overline{10}$ messenger as compared to a copy of $5 \oplus \bar{5}$ messenger field.

The spectrum changes in accordance with the messenger sector. In Ref.[55, 56] expressions for soft masses were derived without considering any model for the messenger and the hidden sector. This model, as it encompasses all the GMSB models, is known as general gauge mediation or GGM. Expressions for the soft masses are as follows:

$$M_r = \alpha_r B_r, \tag{2.6}$$

$$M^2_{\tilde{a}\,\text{usual}} = \sum_r \alpha_r^2 C_r(a)\, A_r. \tag{2.7}$$

Now we see that instead of one scale Λ there are six dimensionful parameters, B_r and A_r. In principle they can be arbitrary. GGM thus predicts non-universal gauginos without spoiling the gauge coupling unification.

As A-terms are not generated even in GGM, none of the pure GMSB models can explain the Higgs mass with a light stop spectrum. In order to explain the Higgs mass one either requires stop masses $\gtrsim 4$ TeV or maximum mixing in the stop sector [13]. One way of generating mixing term or A-term at the boundary is to consider messenger-matter interactions [18, 57].

2.1 Matter-Messenger Interactions

The idea of extending GMSB models by considering messenger-matter interactions is not new [18, 57]. In particular, to solve the severe μ-B_μ problem in GMSB, one needs to couple the Higgs sector with the messenger sector[58–60]. In Ref. [61], contribution of the messenger-matter interactions to other soft masses and the A-terms was calculated us-

ing wavefunction renormalization technique [62]. After the discovery of the Higgs particle this idea became popular as it can save GMSB models by generating large stop mixing parameter. Several works were presented in this idea [16, 17, 19–21]. In Ref. [1, 2], messenger-matter interactions were classified and thoroughly studied in MSSM. In [1] messengers are assumed to be 1, 5 and 10 dimensional representations of SU(5) and these messengers are interacting with the MSSM SU(5) multiplet-wise. In principle messenger-matter interactions can introduce flavor violation. Peccei-Quinn symmetry was used to suppress the flavor violation as well as to classify the models. The general classification reproduced older models [16–21] and as well as found some new models. On the other hand in Ref.[2] messengers are allowed to interact with MSSM fields by SM multiplet-wise. More recent works in this direction can be found in the Refs.[22–31, 47, 63]. Models with explicit flavour violation can be found in [31, 64].

Messenger-matter interactions are classified into two types depending on the number of matter fields in the interaction: (a) Type I where one matter field interacts with two messenger fields, and (b) Type II where one messenger field interacts with two matter fields. Superpotentials for these two types are given as:

$$W_{\rm mix} = \begin{cases} \frac{1}{2}\lambda_{aAB}\Phi_a\Phi_{Am}\Phi_{Bm} & \text{Type I}, \\ \frac{1}{2}\lambda_{abA}\Phi_a\Phi_b\Phi_{Am} & \text{Type II}, \end{cases} \tag{2.8}$$

where $a, b, c\cdots$ is used to indicate visible sector fields and the capital indices $A, B, C, \cdots$ are used to indicate messenger fields. Because of presence of these couplings, one gets 1-loop correction to the soft scalar mass-squared as follows

$$\delta_{\text{1-loop}} M^2_{\tilde{a}} = -\frac{x^2\Lambda^2 h(x)}{96\pi^2} \begin{cases} \sum_{BC} d_a^{BC}\,|\lambda_{aBC}|^2 \,\text{Type I}, \\ \\ \sum_{bB} d_a^{bB}\,|\lambda_{abB}|^2 \,\text{Type II}, \end{cases} \tag{2.9}$$

$d_{\rm indices}$ is a group theoretical factor which appears in beta functions and $h(x)$ has the following form:

$$h(x) = 3\frac{(x-2)\ln(1-x)}{x^4} + (x \to -x). \tag{2.10}$$

Note that 1-loop correction is always negative and it contributes only to the fields which are directly coupled to the messenger fields. Another point is that these contribution are suppressed for small values of $x \lesssim 0.1$ and dominant for $x \sim 0.5$. The A-terms and 2-loop corrections are usually calculated using wavefunction renormalization technique[2, 61, 62]. For Type I and Type II models these corrections are as follows [2]:

Type I models

$$A_a = -\frac{1}{8\pi}\sum_{B,C} d_a^{BC}|\alpha_{aBC}|\,\Lambda, \tag{2.11}$$

$$\delta_{\text{2-loop}}M_{\tilde{a}}^2 = \frac{1}{16\pi^2}\Big[\sum_{B,C,D,c} d_a^{BC}d_B^{cD}|\alpha_{aBC}||\alpha_{cBD}| + \frac{1}{4}\sum_{B,C,D,E} d_a^{BC}d_a^{DE}|\alpha_{aBC}||\alpha_{aDE}| - \frac{1}{2}\sum_{B,C,c,d} d_a^{cd}d_c^{BC}|\alpha_{acd}||\alpha_{cBC}| - \sum_{B,C} d_a^{BC}C_r^{aBC}\alpha_r|\alpha_{aBC}|\Big]\,\Lambda^2, \tag{2.12}$$

where we used α_{indices} to denote $\lambda^2_{\text{indices}}/4\pi$.

Type II models

$$A_a = -\frac{1}{4\pi}\sum_{B,c} d_a^{cB}|\alpha_{acB}|\,\Lambda, \tag{2.13}$$

$$\begin{aligned}\delta_{\text{2-loop}}M_{\tilde{a}}^2 = \frac{1}{16\pi^2}\Big[&\frac{1}{2}\sum_{B,c,d,e} d_a^{cB}d_B^{de}|\alpha_{acB}||\alpha_{deB}| + \sum_{B,C,c,d} d_a^{cB}d_c^{dC}|\alpha_{acB}||\alpha_{cdC}| \\ &+ \sum_{B,C,c,d} d_a^{cB}d_a^{dC}|\alpha_{acB}||\alpha_{adC}| - \sum_{B,c,d,f} d_a^{cd}d_c^{fB}|\alpha_{acd}||\alpha_{cfB}| \\ &+ \frac{1}{32\pi^2}\sum_{B,c,d,e,f} d_a^{cd}d_c^{ef}y^*_{acd}y_{cef}\lambda_{adB}\lambda^*_{efB} + \frac{1}{32\pi^2}\sum_{B,c,d,e,f} d_a^{cB}d_B^{ef}\lambda^*_{acB}\lambda_{efB}y_{acd}y^*_{def} \\ &- 2\sum_{B,c} d_a^{cB}\left(C_r^a + C_r^c + C_r^B\right)\alpha_r|\alpha_{acB}| + \frac{1}{2}\sum_{B,c,e,f} d_a^{cB}d_c^{ef}|\alpha_{cef}||\alpha_{acB}|\Big]\,\Lambda^2.\end{aligned} \tag{2.14}$$

Thus the total soft masses at the boundary are

$$M_{\tilde{a}}^2 = M_{\tilde{a}\,\text{usual}}^2 + \delta_{\text{1-loop}}M_{\tilde{a}}^2 + \delta_{\text{2-loop}}M_{\tilde{a}}^2. \tag{2.15}$$

3 Messenger-matter interactions involving leptons and neutrinos

Before studying the messenger-matter mixing terms involving leptonic fields and right handed neutrinos, we are going to review the inverse seesaw model.

3.1 Inverse seesaw model

The canonical seesaw mechanism requires extension of the MSSM with a heavy field which could be right handed neutrino or triplet Higgs or a triplet fermion (for a review see [65]). The smallness of the neutrino mass is associated with the heaviness of the additional particle. In the canonical seesaw mechanism, the corrections to the Higgs mass are typically very tiny as the right handed neutrino scale is very heavy $\geq 10^{14}$ GeV. Presence of matter messenger mixing terms will not improve the situation. Note that the right handed neutrino (N^c) mass must be less than the messenger scale, otherwise at the messenger scale, N^c fields will be integrated out and messenger-matter interactions involving N^c will now reduce to higher dimensional operator at the messenger scale. If we get any trilinear scalar coupling

from these operators then they must be suppressed not only by the N^c mass but also from loop factors. However, for N^c mass up to 10^5 GeV, the allowed value of the Yukawa coupling (y_N) can be utmost 10^{-5} to get neutrino mass of $\mathcal{O}$(eV). Because of such a small value of y_N, contribution to the Higgs mass from the neutrino sector is negligibly small.

The situation drastically improves in inverse seesaw model [66]. Supersymmetric version of this model has the following superpotential [51, 67]:

$$\begin{aligned} W &= U^c \mathbf{Y_u} Q H_u - D^c \mathbf{Y_d} Q H_d - E^c \mathbf{Y_e} L H_d + \mu H_u H_d \\ &+ N^c y_N L H_u + m_R N^c S + \frac{1}{2}\mu_s S^2, \end{aligned} \tag{3.1}$$

where the MSSM fields are in standard notation with $\mathbf{Y_u}$ etc, representing the Yukawa matrices for three generations and the N^c and S are new fields added to the MSSM field content. These are singlet scalar superfields. Note that if we set μ_s to zero, the above superpotential enjoys U(1) lepton number symmetry. Its presence implies that this symmetry is softly broken. As $\mu_s \to 0$ restores the symmetry, it can be (technically) naturally small. In the above superpotential we have considered only one generation (third) for the inverse seesaw sector. The generalisation to three generations is straight forward and has minor impact on our analysis.

In the basis $\{\nu_L, N^c, S\}$, the mass matrix M_ν of the neutral leptons for one generation, is given by

$$M_\nu = \begin{pmatrix} 0 & m_D & 0 \\ m_D & 0 & m_R \\ 0 & m_R & \mu_s \end{pmatrix}, \tag{3.2}$$

where $m_D = y_N \langle H_u \rangle$. The eigenvalues of the above mass matrix are as follows:

$$\begin{aligned} m_{\nu_1} &\approx \frac{m_D^2\, \mu_s}{m_R^2}, \\ m_{\nu_2} &\approx -\left(\frac{m_D^2}{2\, m_R} + m_R\right), \\ m_{\nu_3} &\approx \left(\frac{m_D^2}{2\, m_R} + m_R\right). \end{aligned} \tag{3.3}$$

Here m_{ν_1}, the lightest neutrino eigenvalue, is proportional to the parameter μ_s. From electroweak precision data [68], $m_D \lesssim 0.05\ m_R$ and thus last two eigenvalues of the mass matrix are degenerate. As m_D and m_R related, y_N and m_R are also related:

$$y_N = \sqrt{\frac{m_{\nu_1}}{\mu_s}}\frac{\sqrt{2}}{v}\mathrm{cosec}\beta\, m_R, \tag{3.4}$$

where v is the electroweak VEV of the Higgs fields: $v = \sqrt{\langle H_u \rangle^2 + \langle H_d \rangle^2} = 246$ GeV. For a fixed μ_s, which we fix it to be electron mass, we see that y_N scales as m_R.

The scalar potential for this model is given below which contains SUSY preserving as

well as SUSY breaking soft terms:

$$V_S = V_F + V_D + V_{\rm soft}, \tag{3.5}$$

where

$$\begin{aligned} V_F &= |Y_e \tilde{E}^c H_d + y_N H_u \tilde{N}|^2 + |Y_u \tilde{Q}\tilde{U}^c + \mu H_d + y_N \tilde{L}\tilde{N}^c|^2 + |y_N \tilde{L} H_u + m_R \tilde{S}|^2 \\ &+ |m_R \tilde{N}^c + \mu_s \tilde{S}|^2 + \dots, \end{aligned} \tag{3.6}$$

$$V_D = \frac{1}{8}(g^2 + g'^2)\,(|H_u|^2 - |H_d|^2), \tag{3.7}$$

$$V_{\rm soft} = A_N y_N \tilde{L} H_u \tilde{N}^c + B_R \tilde{N}^c \tilde{S} + B_S \tilde{S}^\dagger \tilde{S} + h.c. + M_N \tilde{N}^{c\dagger} \tilde{N}^c + \cdots . \tag{3.8}$$

To calculate the neutrino-sneutrino correction to Higgs mass, one needs to calculate the sneutrino mass matrix which has the form:

$$\mathcal{M}^2_{\tilde{\nu}} = \begin{pmatrix} M^2_{\tilde{L}} + D_L + m^2_D & m_D\,(A_N - \mu \cot\beta) & m_R\, m_D \\ * & m^2_D + M^2_N + m^2_R & B_R + m_R\,\mu_s \\ * & * & m^2_R + \mu^2_s + m^2_{\tilde{S}} \end{pmatrix}, \tag{3.9}$$

where the basis is $\{\tilde{\nu}_L, \tilde{N}^c, \tilde{S}\}$, $M^2_{\tilde{L}}$ is the slepton mass, and $m_{\tilde{S}}$ is the soft mass of S. As the mass matrix is symmetric, terms omitted can be easily understood. As the field N^c and S are gauge singlets, soft masses B_R, B_S and M_N are zero at the boundary, the messenger scale. Assuming these are small and $m_D/m_R < 1$, one obtains the following eigenvalues [52]:

$$\begin{aligned} m^2_{\tilde{\nu}_1} &\approx M^2_{\tilde{L}} + m^2_D \left(1 + \frac{m^2_R}{d_2} + \frac{X^2_N}{d_1}\right), \\ m^2_{\tilde{\nu}_2} &\approx M^2_N + m^2_R + m^2_D \left(1 - \frac{X^2_N}{d_1}\right), \\ m^2_{\tilde{\nu}_3} &\approx m^2_{\tilde{S}} + m^2_R - \frac{m^2_R\, m^2_D}{d_2}, \end{aligned} \tag{3.10}$$

where

$$d_1 = M^2_{\tilde{L}} - M^2_N - m^2_R, \tag{3.11}$$

$$d_2 = M^2_{\tilde{L}} - m^2_R - m^2_{\tilde{S}}, \tag{3.12}$$

$$X_N = A_N - \mu \cot\beta\,. \tag{3.13}$$

To compute the corrections to the Higgs mass, we use the effective potential method [69]. The one-loop effective potential for neutrino-sneutrino sector is [51, 52]:

$$V^{\nu/\tilde{\nu}}_{1-loop}(Q^2) = \frac{2}{64\pi^2}\left[\sum_{i=1}^{3} m^4_{\tilde{\nu}_i}\left(\log\frac{m^2_{\tilde{\nu}_i}}{Q^2} - \frac{3}{2}\right) - \sum_{i=1}^{3} m^4_{\nu_i}\left(\log\frac{m^2_{\nu_i}}{Q^2} - \frac{3}{2}\right)\right], \tag{3.14}$$

where first and second term represent the contribution of sneutrino and neutrino mass

eigenstates respectively. An overall factor 2 takes care of the degrees of freedom for the complex scalar and Weyl fermion. The complete calculation of the correction to the Higgs mass is given in the Appendix A. It should be noted that the calculation presented in Appendix A is a slight generalisation of the one presented in Ref. [52] as we relaxed the assumption that X_N is a small parameter.

Without going into details of sneutrino-neutrino sector corrections to the Higgs mass, we can make the following observations:

1. If $m_R >> M_{SUSY}$, the sneutrino (Eq. (3.10)) and neutrino (Eq. (3.3)) eigenvalues are degenerate and are of order of m_R. There will be a complete cancellation between the scalar and fermion sector contributions and consequently no significant correction to the Higgs mass.

2. To have a significant corrections to the Higgs mass, one should have heavy sleptons[52]. In this case the degeneracy between the scalar and fermion eigenvalues breaks and therefore cancellation will not be exact. Since these corrections are inversely proportional to $d_{1,2}$, for heavy sleptons (comparable to m_R), $d_{1,2}$ will be small and consequently one will get significant enhancement to the Higgs mass. Such large sleptons masses can be generated in a framework like general gauge mediation. An alternative way of enhancing the Higgs mass is through matter-messenger corrections which can generate a large X_N parameter and/or significant corrections to $M^2_{\tilde{L}}$. In this case, the sneutrino derivatives are now proportional to X_N (see Appendix A for explicit expressions), the sneutrino contribution will be more as compared to neutrino contribution.

Both the above conditions (large X_N and very heavy sleptons) are not met in the minimal gauge mediation model. Thus the Higgs mass corrections remain small. Clearly both the scenarios with enhanced corrections are not applicable in minimal GMSB. One could however argue to increase the messenger scale, but this would only increase the mass of the stops which is contrary of our philosophy of keeping stops light.

The possibility of increasing the sneutrino/neutrino contributions by increasing the slepton mass in a general gauge mediation model was discussed in Ref. [52]. In the present work, we discuss the importance of the combination of heavy sleptons and large X_N parameter (generated through matter-messenger mixing).

3.2 Classification of the models

We are interested to study the effect of messenger-matter interaction in the inverse seesaw mechanism. We know that the Lagrangian given in Eq. (3.1) has softly broken U(1) lepton number and the softly broken parameter, μ_s, is responsible for the generation of neutrino mass through inverse seesaw. If messenger-matter interactions do not obey U(1) lepton number then we cannot guarantee that inverse seesaw is the only source of neutrino mass. Therefore we impose U(1) lepton number on the messenger fields. To generate A_t and/or A_N, at least one of the fields Q, U^c, H_u, L and N^c has to couple with the messenger fields. Models involving N^c field in the messenger-matter interaction are not explored in the

Model No	Interaction	Lepton number	Remarks or Source
Models with N^c			
1.	$N^c Q \bar{Q}_m$	1	$\in \overline{10}$
2.	$N^c U^c \bar{U}^c_m$	1	$\in \overline{10}$
3.	$N^c D^c \bar{D}^c_m$	1	$\in 5$
4.	$N^c L H^m_u$	0	$\in 5$
5.	$N^c E^c \bar{E}^c_m$	2	$\in \overline{10}$
6.	$N^c H_u H^m_d$	1	$\in \bar{5}$
7.	$N^c H_d H^m_u$	1	$\in 5$
8.	$\frac{1}{2}(N^c)^2 S_m$	2	$\in 1$
9.	$N^c S S_m$	0	$\in 1$
10.	$N^c H^m_u H^m_d$	$--$	$\in 5 \oplus \bar{5}$
Models with L			
11.	$L Q D^c_m$	-1	$\in \bar{5}$
12.	$L D^c Q_m$	-1	$\in 10$
13.	$L E^c H^m_d$	0	$\in \bar{5}$
14.	$L H_d E^c_m$	-1	$\in 10$
15.	$L H_u S_m$	-1	$\in 1$
16.	$L S H^m_u$	-2	$\in 5$
17.	$L H^m_u S_m$	$--$	$\in 1, 5$

Table 1. Classification of the models. Note that, for the models 1, 2, 5 and 14, messenger fields are $10 \oplus \overline{10}$ and for the rest of the models these are $5 \oplus \bar{5}$. Each model contains only one term and the corresponding coupling is chosen to be λ. In the third column lepton number of the messenger fields are listed. As in the model 10 and 17 two messenger fields are appearing in each interaction terms, one can assign any lepton number to the messengers keeping in mind that product of their lepton numbers should be 1 and -1 for the model 10 and 17 respectively. In the last column we mention the representation and source of the messenger field or fields.

literature. We have listed 17 possible models of messenger-matter interactions involving L and N^c fields in Table 1. In these models we allow only the third generation of the matter fields to couple with the messenger fields. The interaction term $L^2 E^c_m$ is not there in the above list because this vanishes. Along with the interaction terms listed above, some new terms may be allowed by symmetry. For example, in model 5, the term $S^2 E^c_m$ is allowed. However, we are not considering this term as it will not generate A_t or A_N. For the same reason, we do not list the models involving only E^c or S. Each of the model contains the shown interaction in the superpotential. Inter-generational mixing is considered to be absent. When more than one messenger fields is considered, the matter-messenger coupling is considered universal over all the messenger fields.

Some of the models involving L, like model 11, 13 and 15, are not new. These are

considered in Ref. [1] along with other interaction terms. As mentioned earlier, the suffix m is used to indicate messengers. Messenger field with known symbol has the same quantum number under SM gauge group. Here models 10 and 17 are Type I models and rest of the models are of Type II. In each model we are allowing only one messenger-matter interaction term. In the next section, we are going to list the modification of the boundary conditions due to these messenger-matter interactions.

4 Analysis of the models

From the previous section it is clear that the fields which are coupled with the messenger fields through Yukawa interactions have negative one-loop corrections as well as positive two-loop corrections to their soft masses. Other matter fields which are not directly coupled to the messenger fields but, have Yukawa interactions with the matter fields with direct interactions to the messenger fields, always get two-loop negative contributions. On the top of these corrections, there are usual GMSB contributions to the soft masses which are always positive. The messenger-matter coupling λ cannot take arbitrary values as it can lead to negative mass squared eigenvalues for the scalars at the weak scale.

Another important parameter is $x \equiv \Lambda/M$. One-loop corrections diminish for smaller values of x. We consider two cases: (a) $x = 0.5$ for which we cannot neglect 1-loop effects, and (b) $x = 0.1$ for which 1-loop contributions can be neglected.

Because of non-observation of any SUSY particle, LHC bounds on the soft masses are very stringent. In GGM models, the present lower limits on gluino is 1.6 TeV [70], whereas on the chargino it is 650 GeV [71]. It can be easily seen that LHC bound on chargino mass is more stronger than that of the gluino mass in the universal gaugino mass case. If one considers mGMSB with $N = d = 1$ then the upper bound on the gluino mass forces the stop masses to be of the order of 2 TeV. However one could be interested in light spectrum for various reasons including the fine-tuning issue. To resolve this issue in the models with $5 \oplus \bar{5}$, we consider the number of messengers to be 3. In models 1, 2, 5 and 14 this problem is automatically solved as $10 \oplus \overline{10}$ messenger field has $d = 3$. We choose the following values in the numerical analysis:

	$5 \oplus \bar{5}$	$10 \oplus \overline{10}$
Models	$3, 4, 6, 7, \cdots, 11, 13, 15, 16, 17$	$1, 2, 5, 12, 14$
Λ	100 TeV	100 TeV
Number of messengers	3	1
Dynkin index	1	3

(4.1)

Gravitino is the LSP in these models. Its mass has the following expression:

$$m_{\frac{3}{2}} = \frac{F}{\sqrt{3}M_{\rm Pl}} = \frac{\Lambda^2}{\sqrt{3}xM_{\rm Pl}} = \frac{10}{4.16x}\,\text{eV}, \tag{4.2}$$

where $M_{\rm Pl} = 2.4 \times 10^{18}$ GeV. Thus we get gravitino mass 4.8 eV and 24 eV for $x = 0.5$ and $x = 0.1$, respectively. Experimental bound on gravitino mass at 2σ limit is 16 eV

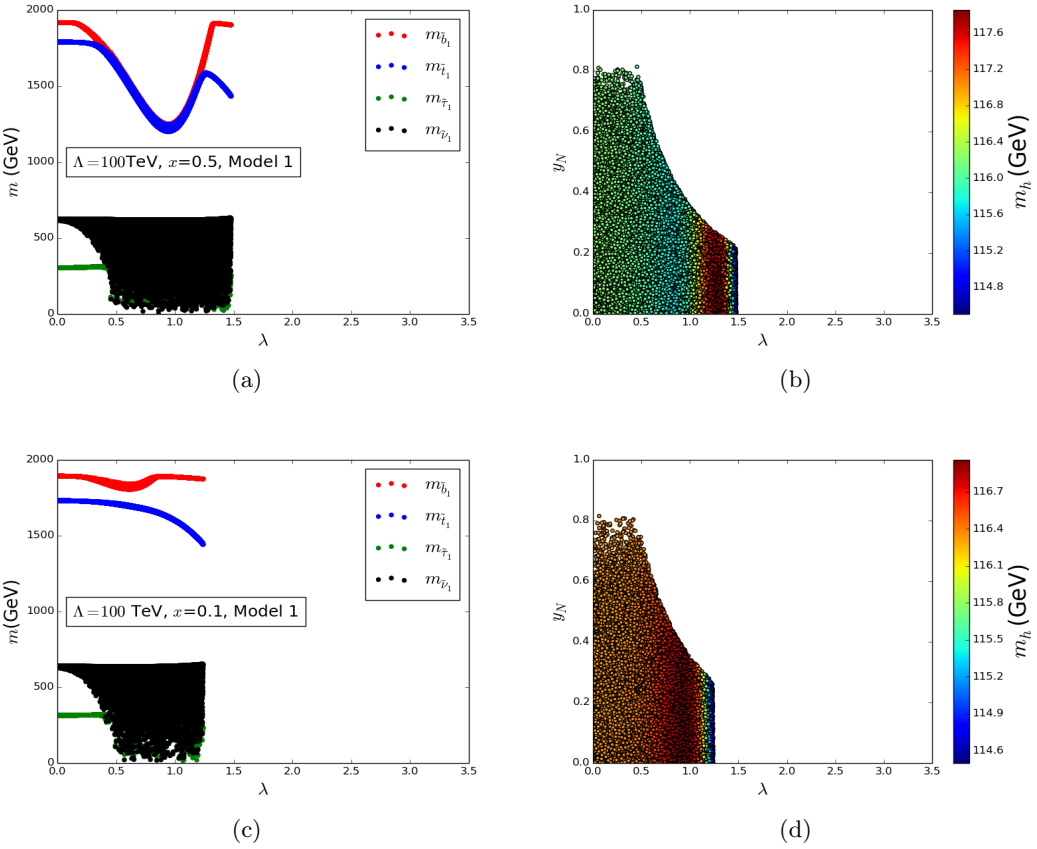

Figure 1. Model 1: Variation of the third generation soft masses with messenger-matter interaction coupling λ is shown in the left panel, and Higgs mass values in λ and y_N plane are shown in the right panel. The upper and lower plots correspond to $x = 0.5$ and $x = 0.1$ respectively.

[72]. Though $x = 0.1$ case is ruled out by gravitino mass constraint, there is a way out to overcome this gravitino problem [73].

Lepton number violating mass parameter μ_s is another important parameter. Upper limit of y_N depends on it. The upper bound on y_N comes from electroweak precision tests, which sets the ratio $m_D/m_R < \frac{1}{20}$ [68]. We consider $\mu_s = 5 \times 10^{-4} m_e$, this fixes the m_D/m_R ratio to be of the $\frac{1}{70}$ for a neutrino mass of 10^{-1} eV. And thus the limits from electroweak precision tests are always satisfied. As $y_N \propto \text{cosec}\beta$, it is insensitive to β for higher values of $\tan\beta$. We thus kept $\tan\beta = 10$ through out the analysis. For spectrum calculation, a modified version of the publicly available code SuSeFLAV [74] is used. All the low energy phenomenological constraints including flavour constraints dominantly from $BR(B \to X_s + \gamma)$ and mass constraints from LHC are imposed on the spectrum. We will now discuss each model in detail.

4.1 Model 1

Model 1 is a Type II model of our classification which interacts with the quark doublet fields and the singlet. $W_{\text{mix}} = \lambda N^c Q \bar{Q}_m$, the resultant one-loop and two-loop corrections

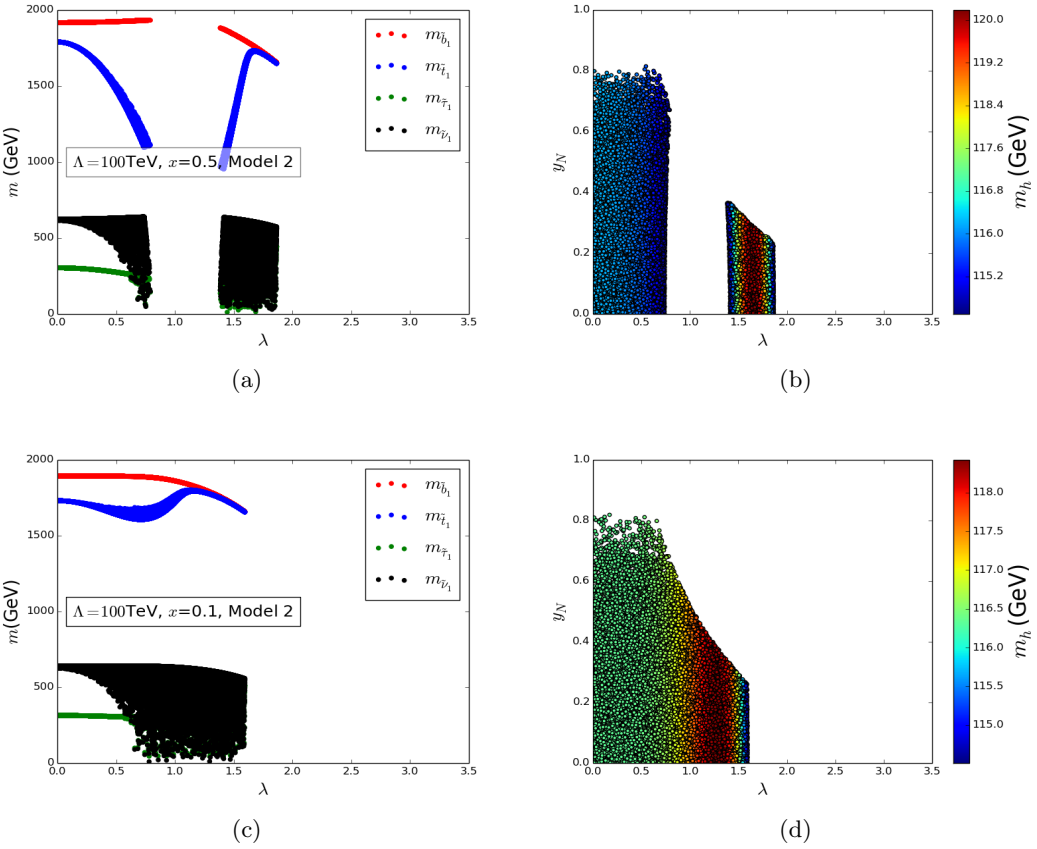

Figure 2. Model 2: Upper two plots correspond to $x = 0.5$ and the lower two are for $x = 0.1$. Note that depth of blue line is higher for this model compared to model 1. Please see caption of Fig. 1 for details of notation.

to the various soft masses are shown below

$$\delta M^2_{\tilde{Q}} = \Big[-\frac{\alpha_\lambda}{24\pi} x^2 h(x) + \frac{\alpha_\lambda \left(-\alpha_1 + 5\left(-9\alpha_2 - 16\alpha_3 + 6\alpha_N + 24\alpha_\lambda\right)\right)}{240\pi^2} \Big] \Lambda^2$$

$$\delta M^2_{\tilde{U}^c} = \Big[-\frac{\alpha_t \alpha_\lambda}{8\pi^2} \Big] \Lambda^2$$

$$\delta M^2_{\tilde{D}^c} = \Big[-\frac{\alpha_b \alpha_\lambda}{8\pi^2} \Big] \Lambda^2$$

$$\delta M^2_{\tilde{L}} = \Big[-\frac{3\alpha_N \alpha_\lambda}{8\pi^2} \Big] \Lambda^2$$

$$
\begin{aligned}
\delta M^2_{\tilde{N}^c} &= \Big[-\frac{\alpha_\lambda}{4\pi} x^2 h(x) + \frac{\alpha_\lambda \left(-\alpha_1 + 5\left(-9\alpha_2 - 16\alpha_3 + 3\left(\alpha_b + \alpha_t + 8\alpha_\lambda\right)\right)\right)}{40\pi^2} \Big] \Lambda^2 \\
\delta M^2_{H_u} &= \Big[-\frac{3\left(\alpha_t + 2\alpha_N\right)\alpha_\lambda}{16\pi^2} \Big] \Lambda^2 \\
\delta M^2_{H_d} &= \Big[-\frac{3\alpha_b \alpha_\lambda}{16\pi^2} \Big] \Lambda^2 \\
\delta A_t &= \Big[-\frac{\alpha_\lambda}{4\pi} \Big] \Lambda \\
\delta A_b &= \Big[-\frac{\alpha_\lambda}{4\pi} \Big] \Lambda \\
\delta A_N &= \Big[-\frac{3\alpha_\lambda}{2\pi} \Big] \Lambda,
\end{aligned} \tag{4.3}
$$

where

$$
\alpha_t = \frac{y_t^2}{4\pi},\ \alpha_b = \frac{y_b^2}{4\pi},\ \alpha_\tau = \frac{y_\tau^2}{4\pi},\ \alpha_\lambda = \frac{\lambda^2}{4\pi} \text{ and } \alpha_N = \frac{y_N^2}{4\pi}. \tag{4.4}
$$

In this model $\tilde{Q}$ and $\tilde{N}^c$ get one-loop negative corrections to their masses. For $x = 0.5$, the interplay between the one-loop, two-loop corrections and the standard GMSB contributions is clearly evident in the lightest stop and sbottom masses shown in Fig. 1 (a). As can be seen, when λ is relatively small, the negative one-loop contributions significantly cancel with the standard GMSB contributions, lowering the lightest eigenvalue to smaller values. The cancellation is maximum around $\lambda \sim 1$. Beyond those values of λ, positive two-loop contributions start dominating over the one-loop contributions resulting in positive and larger spectra. For $x = 0.1$ the one-loop effects are no longer important and the cancellation regions disappear as can be seen from the Fig 1(c). For both the cases, as λ increases, staus and stops start becoming tachyonic for values $\lambda \gtrsim 1.5$. Remember that the staus receive negative contributions at two-loops from matter-messenger mixing terms at the messenger scale (Eq. 4.3).

The Higgs mass values for the allowed parameter space are presented for $x = 0.5$ in Fig. 1(b) and for $x = 0.1$ in Fig. 1(d). This model can not produce the correct Higgs mass because although both A_t and A_N are generated but sleptons are not that heavy. However A_N is dominant over A_t by a factor three as can be seen from Eq. (4.3). To disentangle the effects from each contribution, we use three different notations to illustrate the corrections to the Higgs mass. We used m_h^0 parameter for pure MSSM Higgs mass, $m_h^{0+\Delta}$ denotes Higgs mass, calculated including the matter messenger mixing terms in the boundary conditions but without considering the corrections from the neutrino-sneutrino sector, on the top of the MSSM and m_h is the actual Higgs mass when all the corrections are considered.

Four benchmark points (two each with $x = 0.5$ and $x = 0.1$) are presented in Table 2. As can be seen from the benchmark points, even both A_t and A_N are not sufficient to provide correct Higgs mass. The stop spectrum is relatively light ~ 1.7 TeV. The sneutrino mixing parameter A_N is relatively large compared to the A_t generated.

Parameter	x = 0.5	x = 0.5	x = 0.1	x = 0.1	Parameter	x = 0.5	x = 0.5	x = 0.1	x = 0.1
λ	1.34	0.53	0.55	0.55	y_N	0.24	0.51	0.51	0.21
A_N	-6650.7	-1021.8	-1074.6	-1136.3	A_t	-1477.9	-727.3	-829.4	-843.4
m_R	5823.8	6195.3	6469.5	3732.3	μ	1400.	790.	935.	823.
$m_{\tilde{\nu}_1}$	133.	441.	426.	610.	$m_{\tilde{\nu}_{2,3}}/m_{\nu_{2,3}}$	5824.	6196.	6470.	3732.
m_h	117.05	115.62	116.06	117.21	m_H	1523.	1003.	1129.	999.
$m_h^{0+\Delta}$	117.05	115.60	116.04	117.21	m_{A^0}	1539.	1013.	1141.	1001.
m_h^0	115.84	115.84	116.18	116.18	$m_{H^\pm}$	1541.	1016.	1144.	1003.
M_S	1728.	1706.	1768.	1759.	$m_{\tilde{g}}$	2187.	2180.	2108.	2108.
$\tilde{t}_1$	1561.	1611.	1707.	1703.	$\tilde{t}_2$	1913.	1806.	1832.	1816.
$\tilde{b}_1$	1912.	1620.	1831.	1809.	$\tilde{b}_2$	1926.	1928.	1899.	1888.
$\tilde{\tau}_1$	119.	317.	316.	311.	$\tilde{\tau}_2$	299.	321.	323.	324.
$\tilde{u}_1$	1935.	1916.	1897.	1892.	$\tilde{u}_2$	2003.	1936.	1909.	1910.
$\tilde{d}_1$	1927.	1931.	1901.	1902.	$\tilde{d}_2$	1993.	1931.	1902.	1902.
$\tilde{e}_1$	299.	321.	323.	324.	$\tilde{e}_2$	311.	446.	432.	614.
N_1	431.	430.	412.	412.	N_2	822.	749.	772.	750.
N_3	1408.	795.	942.	829.	N_4	1413.	878.	965.	873.
C_1	806.	740.	758.	739.	C_2	1404.	863.	955.	862.

Table 2. Model 1: Matter-messenger mixing parameter, neutrino sector parameters, Higgs mass and SUSY spectrum for the benchmark points from $x = 0.5$ and $x = 0.1$ cases. In each case the considered benchmark represents small and large allowed λ range. Here m_h^0 means pure MSSM Higgs mass calculated at the two-loop level, $m_h^{0+\Delta}$ is the Higgs mass when all the mixing terms except the neutrino mixing are considered on the top of the MSSM and m_h is the actual Higgs mass when all the corrections were considered. All the masses are given in GeV. The Λ values are taken as in Eq. (4.1).

4.2 Model 2

This model has similar structure as Model 1 with quark doublets replaced by the up type quark singlet. The resultant one-loop and two-loop corrections are listed below in Eq.4.5

$$\begin{aligned}
\delta M^2_{\tilde{Q}} &= \Big[-\frac{\alpha_t \alpha_\lambda}{16\pi^2} \Big] \Lambda^2 \\
\delta M^2_{\tilde{U}^c} &= \Big[-\frac{\alpha_\lambda}{24\pi} x^2 h(x) + \frac{\alpha_\lambda \left(-16\alpha_1 - 80\alpha_3 + 30\alpha_N + 75\alpha_\lambda\right)}{240\pi^2} \Big] \Lambda^2 \\
\delta M^2_{\tilde{L}} &= \Big[-\frac{3\alpha_N \alpha_\lambda}{16\pi^2} \Big] \Lambda^2 \\
\delta M^2_{\tilde{N}^c} &= \Big[-\frac{\alpha_\lambda}{8\pi} x^2 h(x) + \frac{\alpha_\lambda \left(-16\alpha_1 - 80\alpha_3 + 30\alpha_t + 75\alpha_\lambda\right)}{80\pi^2} \Big] \Lambda^2 \\
\delta M^2_{H_u} &= \Big[-\frac{3\left(\alpha_t + \alpha_N\right)\alpha_\lambda}{16\pi^2} \Big] \Lambda^2 \\
\delta A_t &= \Big[-\frac{\alpha_\lambda}{4\pi} \Big] \Lambda \\
\delta A_N &= \Big[-\frac{3\alpha_\lambda}{4\pi} \Big] \Lambda.
\end{aligned} \tag{4.5}$$

Parameter	x = 0.5	x = 0.5	x = 0.1	x = 0.1	Parameter	x = 0.5	x = 0.5	x = 0.1	x = 0.1
λ	1.58	0.66	1.32	0.72	y_N	0.27	0.62	0.36	0.65
A_N	-4599.7	-785.0	-3137.3	-882.2	A_t	-1845.6	-814.3	-1495.5	-925.6
m_R	6162.5	8773.4	7394.6	9977.0	μ	1551.	852.	1527.	1050.
$m_{\tilde{\nu}_1}$	306.	425.	115.	322.	$m_{\tilde{\nu}_{2,3}}/m_{\nu_{2,3}}$	6163.	8774.	7395.	9978.
m_h	119.24	114.84	117.80	116.24	m_H	1671.	1053.	1643.	1217.
$m_h^{0+\Delta}$	119.22	114.82	117.78	116.22	m_{A^0}	1686.	1071.	1662.	1241.
m_h^0	119.22	114.82	115.95	115.94	$m_{H^\pm}$	1688.	1074.	1664.	1244.
M_S	1722.	1569.	1820.	1761.	$m_{\tilde{g}}$	2182.	2184.	2114.	2110.
$\tilde{t}_1$	1600.	1291.	1771.	1666.	$\tilde{t}_2$	1853.	1906.	1871.	1862.
$\tilde{b}_1$	1808.	1928.	1783.	1888.	$\tilde{b}_2$	1922.	1934.	1889.	1901.
$\tilde{\tau}_1$	269.	256.	108.	288.	$\tilde{\tau}_2$	321.	262.	418.	315.
$\tilde{u}_1$	1922.	1948.	1885.	1910.	$\tilde{u}_2$	1935.	1974.	1990.	1927.
$\tilde{d}_1$	1930.	1934.	1896.	1901.	$\tilde{d}_2$	1930.	1959.	1897.	1909.
$\tilde{e}_1$	321.	262.	418.	315.	$\tilde{e}_2$	356.	430.	422.	349.
N_1	431.	430.	413.	412.	N_2	822.	783.	782.	780.
N_3	1559.	858.	1536.	1058.	N_4	1563.	908.	1540.	1071.
C_1	806.	769.	773.	766.	C_2	1554.	895.	1529.	1062.

Table 3. Benchmark points for Model 2. As can be seen, the neutrino corrections can be significant in some regions of the parameter space compared to the matter messenger mixing corrections. See caption of Table 2 for details of notation.

In this case $\tilde{U}^c$ and N^c fields get one-loop negative and two-loop positive contributions to their soft masses. From Figs. 2(a) and 2(c), we can see the variation of the lightest third generation mass eigenvalues with respect to λ. For $x = 0.5$, cancellations only appear for the stop sector and not in the bottom sector as the messenger matter interactions are only active for the up-type singlet sector. The cancellations are however much deeper here as the standard GMSB contributions for the singlet up squarks is lesser compared to the doublet squarks. The cancellation is milder as expected for $x = 0.1$.

In this case A_N dominates A_t by a factor three as in Model 1. For large $\lambda \gtrsim 2$, sneutrinos, stops and sbottoms become tachyonic making the model unviable. The Higgs mass values are presented in Figs. 2(b) and 2(d).

Four benchmark points are given in Table 3, as before two for $x = 0.5$ and two for $x = 0.1$. As can be seen from the points, neutrino/sneutrino contribution is not significant in this model.

4.3 Model 3

Model 3 is a Type II model of our classification in which down quark interacts with a messenger field transforming as a conjugate representation of D^c: $W_{\rm mix} = \lambda N^c D^c \bar{D}^c_m$. The

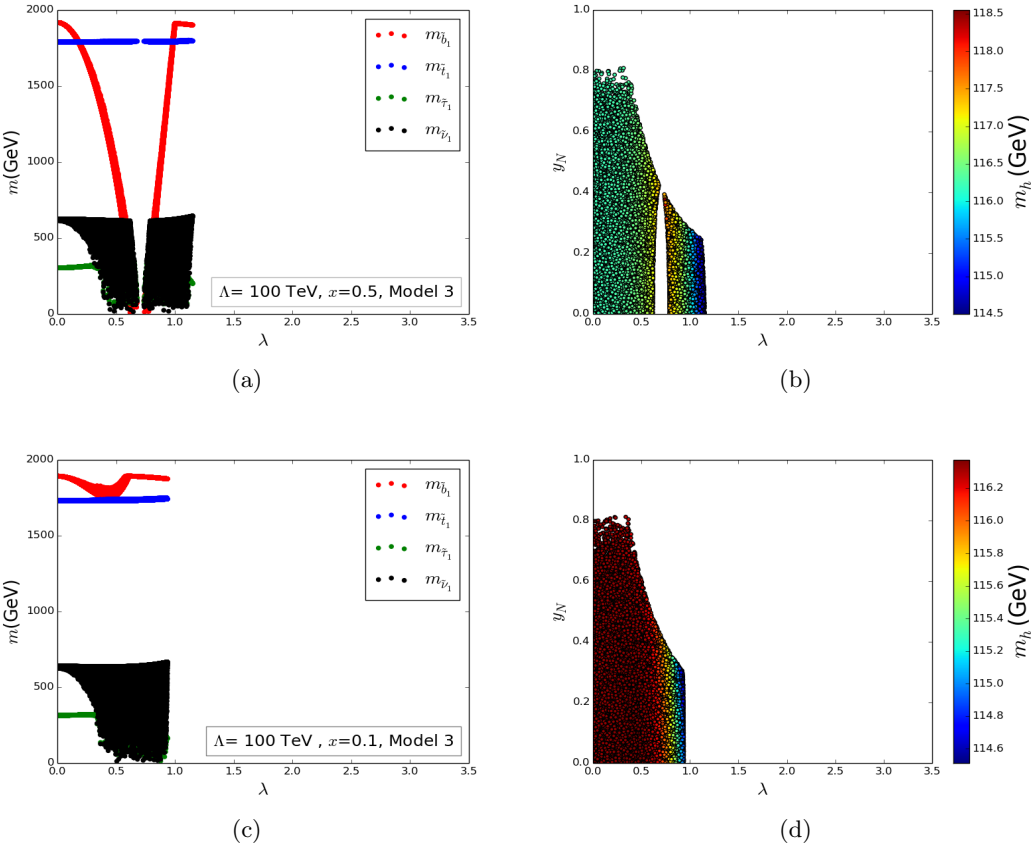

Figure 3. Model 3: Spectrum variation with λ and Higgs mass data points in y_N and λ plane. Note that in (b) origin is not at zero but at 0.7 for λ. Please see caption of Fig. 1 for details of notations.

resultant one-loop and two-loop corrections to the various soft masses are shown below

$$\begin{aligned}
\delta M^2_{\tilde{Q}} &= \Big[-\frac{3\alpha_b\alpha_\lambda}{16\pi^2}\Big]\Lambda^2 \\
\delta M^2_{\tilde{D}^c} &= \Big[-\frac{\alpha_\lambda}{8\pi}x^2h(x) + \frac{\alpha_\lambda\left(-4\alpha_1 - 80\alpha_3 + 30\alpha_N + 195\alpha_\lambda\right)}{80\pi^2}\Big]\Lambda^2 \\
\delta M^2_{\tilde{L}} &= \Big[-\frac{9\alpha_N\alpha_\lambda}{16\pi^2}\Big]\Lambda^2 \\
\delta M^2_{H_u} &= \Big[-\frac{9\alpha_N\alpha_\lambda}{16\pi^2}\Big]\Lambda^2 \\
\delta M^2_{H_d} &= \Big[-\frac{9\alpha_b\alpha_\lambda}{16\pi^2}\Big]\Lambda^2 \\
\delta M^2_{\tilde{N}^c} &= \Big[-3\frac{\alpha_\lambda}{8\pi}x^2h(x) + \frac{3\alpha_\lambda\left(-4\alpha_1 - 80\alpha_3 + 30\alpha_b + 195\alpha_\lambda\right)}{80\pi^2}\Big]\Lambda^2 \\
\delta A_b &= \Big[-\frac{3\alpha_\lambda}{4\pi}\Big]\Lambda \\
\delta A_N &= \Big[-\frac{9\alpha_\lambda}{4\pi}\Big]\Lambda.
\end{aligned} \tag{4.6}$$

Parameter	x = 0.5	x = 0.5	x = 0.1	x = 0.1	Parameter	x = 0.5	x = 0.5	x = 0.1	x = 0.1
λ	0.83	0.41	0.81	0.45	y_N	0.28	0.54	0.32	0.59
A_N	−3921.8	−955.1	−3716.3	−1072.6	A_t	−572.2	−575.5	−679.5	−679.6
m_R	4753.9	8559.6	9412.0	7235.1	μ	803.	770.	937.	905.
$m_{\tilde{\nu}_1}$	330.	421.	273.	325.	$m_{\tilde{\nu}_{2,3}}/m_{\nu_{2,3}}$	4754.	8560.	9412.	7236.
m_h	117.22	116.43	115.48	116.30	m_H	1004.	983.	1111.	1098.
$m_h^{0+\Delta}$	117.20	116.42	115.46	116.27	m_{A^0}	1011.	997.	1135.	1115.
m_h^0	116.23	116.22	116.33	116.33	$m_{H^\pm}$	1014.	1000.	1137.	1117.
M_S	1842.	1842.	1803.	1798.	$m_{\tilde{g}}$	2183.	2182.	2117.	2110.
$\tilde{t}_1$	1792.	1792.	1744.	1738.	$\tilde{t}_2$	1893.	1893.	1864.	1861.
$\tilde{b}_1$	694.	1266.	1885.	1800.	$\tilde{b}_2$	1921.	1923.	1894.	1897.
$\tilde{\tau}_1$	317.	326.	233.	299.	$\tilde{\tau}_2$	344.	332.	259.	324.
$\tilde{u}_1$	1927.	1927.	1912.	1906.	$\tilde{u}_2$	1971.	1971.	1938.	1942.
$\tilde{d}_1$	1926.	1924.	1927.	1899.	$\tilde{d}_2$	1960.	1956.	1994.	1925.
$\tilde{e}_1$	344.	332.	259.	324.	$\tilde{e}_2$	361.	427.	299.	350.
N_1	430.	429.	413.	412.	N_2	756.	736.	772.	768.
N_3	808.	775.	943.	912.	N_4	881.	870.	966.	938.
C_1	747.	727.	759.	755.	C_2	868.	855.	956.	928.

Table 4. Benchmark points for Model 3. See caption of Table 2 for details of notation.

Here $M_{\tilde{D}^c}$ and $M_{\tilde{N}^c}$ get one-loop negative contributions. Cancellation between the one-loop contribution and the two-loop contributions for $M_{\tilde{D}^c}$ is so severe in $x = 0.5$ case that the $m_{\tilde{b}_1}$ becomes tachyonic for $\lambda \approx 0.6 - 0.7$ (Fig. 3(a)). One may wonder why $m_{\tilde{b}_1}$ goes to negative here while $m_{\tilde{t}_1}$ of previous model does not touch the zero line. Note that $\tilde{U}^c$ mass at the boundary is slightly higher than that of $\tilde{D}^c$ because former has hypercharge double of the later one. Hence the cancellation is less severe in model 2. This cancellation is less for $x = 0.1$ as expected (Fig. 3(c)).

In this model, no A_t term is generated at the boundary. We see that parameter space of λ splits into two parts for $x = 0.5$ (Fig. 3(b)) and one can not obtain the correct Higgs mass in this model. For the case of $x = 0.1$, however, parameter space for λ is continuous (Fig. 3(d)) and the spectrum becomes tachyonic for $\lambda > 1.0$. The benchmark points are given in Table 4.

4.4 Model 4

This is a Type II model with messenger matter interaction $W_{\rm mix} = \lambda N^c L H_u^m$. Like the previous model, this model has $5 \oplus \bar{5}$ messengers. One-loop and two-loop contribution to

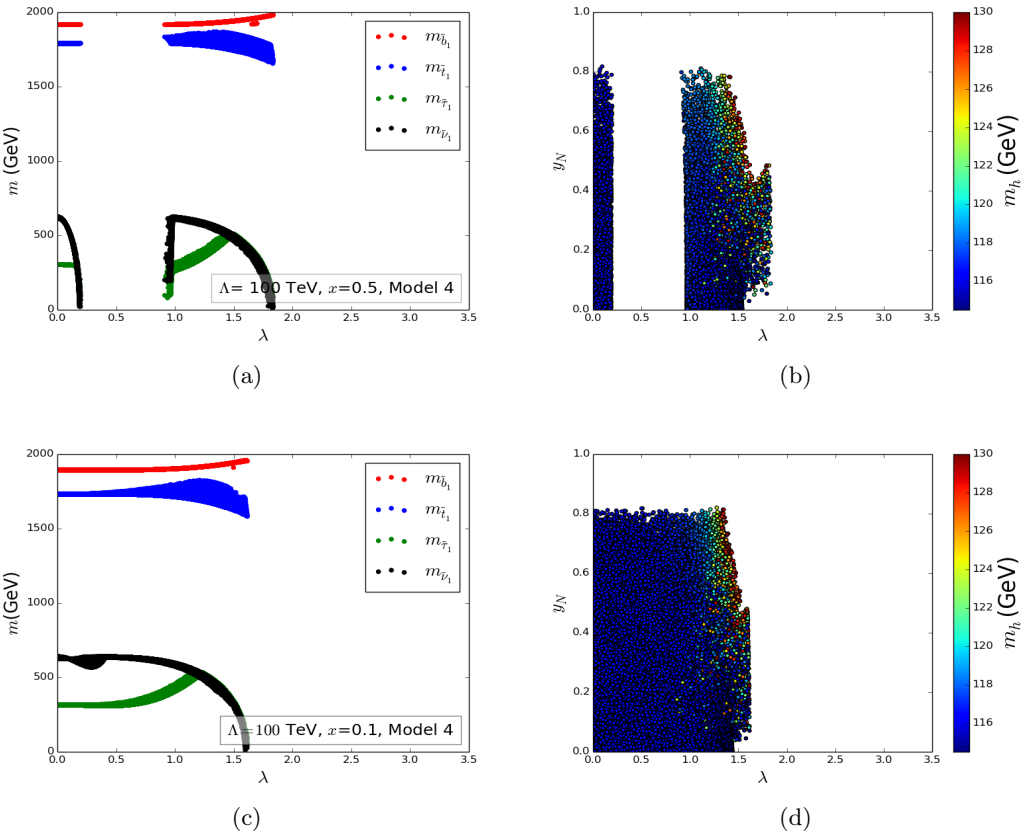

Figure 4. Model 4: Spectrum variation with λ and Higgs mass values in y_N and λ plane. Please see caption of Fig. 1 for details of notation.

the soft masses are shown in Eq. (4.7).

$$\begin{aligned}
\delta M^2_{\tilde{L}} &= \Big[-\frac{\alpha_\lambda}{8\pi}x^2h(x) + \frac{3\alpha_\lambda\left(-3\alpha_1-15\alpha_2+10\left(\alpha_N+5\alpha_\lambda\right)\right)}{80\pi^2}\Big]\Lambda^2\\
\delta M^2_{\tilde{E^c}} &= \Big[-\frac{3\alpha_\lambda\alpha_\tau}{8\pi^2}\Big]\Lambda^2\\
\delta M^2_{H_u} &= \Big[-\frac{9\alpha_N\alpha_\lambda}{16\pi^2}\Big]\Lambda^2\\
\delta M^2_{H_d} &= \Big[-\frac{3\alpha_\lambda\alpha_\tau}{16\pi^2}\Big]\Lambda^2\\
\delta M^2_{\tilde{N^c}} &= \Big[-\frac{\alpha_\lambda}{4\pi}x^2h(x) + \frac{3\alpha_\lambda\left(5\left(-3\alpha_2+2\alpha_N+10\alpha_\lambda+\alpha_\tau\right)-3\alpha_1\right)}{40\pi^2}\Big]\Lambda^2\\
\delta A_\tau &= \Big[-\frac{3\alpha_\lambda}{4\pi}\Big]\Lambda\\
\delta A_N &= \Big[-\frac{9\alpha_\lambda}{4\pi}\Big]\Lambda.
\end{aligned} \tag{4.7}$$

Here $M^2_{\tilde{L}}$ and $M^2_{\tilde{N^c}}$ get one-loop negative contributions and two-loop positive contributions. We know that usual GMSB contributions to the $M^2_{\tilde{L}}$ and $M^2_{\tilde{E^c}}$ are small. Thus in the models

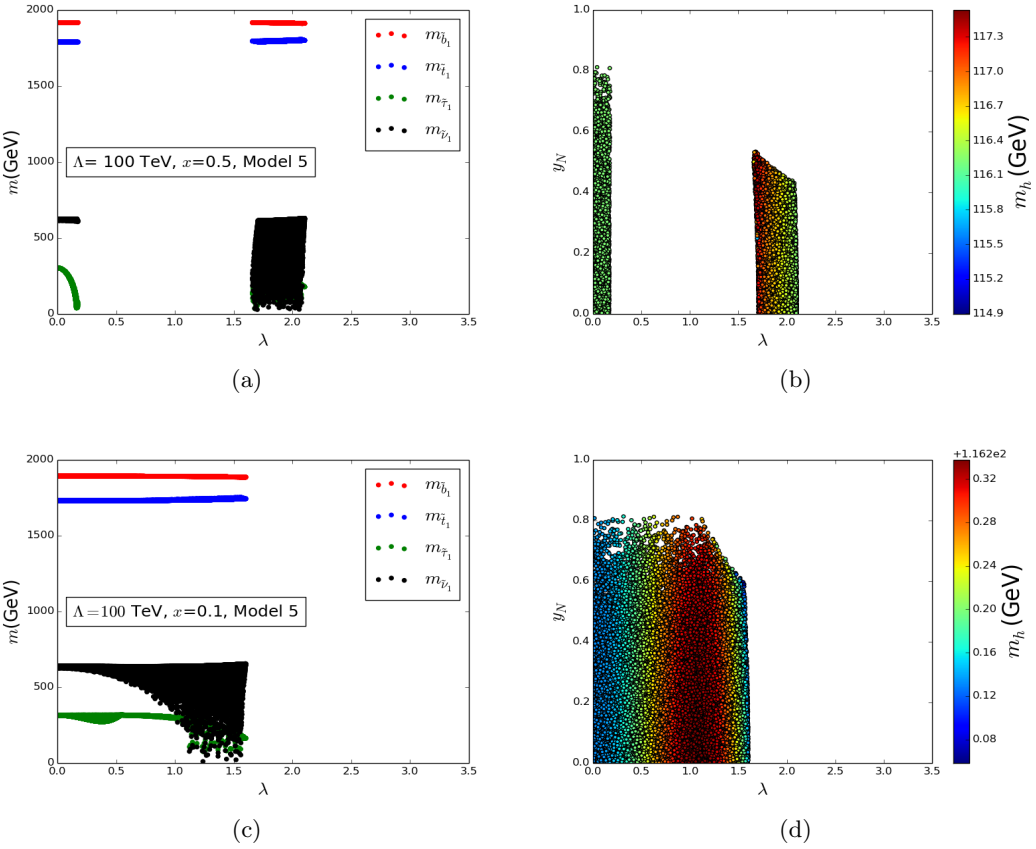

Figure 5. Model 5: Spectrum variation with λ and Higgs mass values in y_N and λ plane. Please see caption of Fig. 1 for details of notation.

where these masses get one-loop negative contributions, $M^2_{\tilde{L}}$ will be large (comparable to m_R). Therefore $d_{1,2}$ (Eq. 3.11 and 3.12) will be small which appear in the denominator of the Higgs mass expressions and enhances the contribution. Therefore one will correct Higgs mass.

In Fig. 4(a) one can see that $m_{\tilde{\tau}_1}$ becomes tachyonic for vary small values of $\lambda \sim 0.18$ and for larger λ one can get positive spectrum. The larger band ($\lambda > 1.0$) has correct Higgs mass. For $x = 0.1$, strength of one-loop contribution diminishes and hence larger values of λ are allowed. Beyond $\lambda = 1.6$, $m_{\tilde{\tau}_1}$ is tachyonic as can be seen in Fig. 4(c). For these values of λ two-loop negative contribution to $M_{\tilde{E}^c}$ dominates over usual GMSB contribution. In the Higgs mass scatter plot (Fig. 4(b) and (d)), one can see that this model is capable of giving correct Higgs mass. From these figures, we can see the importance of m_R parameter. The Higgs mass is sensitive to the m_R value for a given point in the y_N-λ plane. Like the model 3, in this model too A_t term is not generated at the boundary. Hence, A_N and heavy $M^2_{\tilde{L}}$ are mainly responsible for raising the Higgs mass up to the required value. For the $x = 0.5$ case, one need the value of $-A_N$ is ~ 12 to 4 TeV (Table 5) to raise the Higgs mass from its pure MSSM value as shown in Table 5.

Parameter	x = 0.5	x = 0.5	x = 0.1	x = 0.1	Parameter	x = 0.5	x = 0.5	x = 0.1	x = 0.1
λ	1.49	1.18	1.37	0.82	y_N	0.39	0.14	0.46	0.17
A_N	-12389.9	-7925.4	-10240.4	-3869.9	A_t	$-513.$	-578.0	-581.2	-693.0
m_R	7564.6	2891.9	7985.1	2096.7	μ	1624.	743.	1893.	798.
$m_{\tilde{\nu}_1}$	5801.	2732.	6190.	2161.	$m_{\tilde{\nu}_{2,3}}/m_{\nu_{2,3}}$	7567.	2900.	7987.	2079.
m_h	124.93	122.69	125.04	124.53	m_H	1558.	949.	1767.	1011.
$m_h^{0+\Delta}$	112.79	116.08	112.59	116.15	m_{A^0}	1709.	953.	1953.	1013.
m_h^0	116.20	116.2	116.33	116.3	$m_{H^\pm}$	1709.	955.	1953.	1016.
M_S	1821.	1834.	1767.	1789.	$m_{\tilde{g}}$	2189.	2188.	2113.	2111.
$\tilde{t}_1$	1783.	1783.	1727.	1726.	$\tilde{t}_2$	1860.	1887.	1807.	1854.
$\tilde{b}_1$	1939.	1922.	1928.	1897.	$\tilde{b}_2$	1945.	1927.	1936.	1903.
$\tilde{\tau}_1$	501.	324.	436.	350.	$\tilde{\tau}_2$	5804.	2741.	6194.	2139.
$\tilde{u}_1$	1879.	1919.	1827.	1899.	$\tilde{u}_2$	1992.	1971.	1981.	1942.
$\tilde{d}_1$	1945.	1927.	1936.	1903.	$\tilde{d}_2$	1985.	1957.	1975.	1926.
$\tilde{e}_1$	520.	389.	652.	383.	$\tilde{e}_2$	612.	605.	735.	626.
N_1	431.	429.	413.	411.	N_2	824.	716.	791.	738.
N_3	1633.	748.	1893.	803.	N_4	1637.	864.	1895.	861.
C_1	805.	707.	773.	726.	C_2	1626.	847.	1893.	848.

Table 5. Benchmark points for Model 4. See caption of Table 2 for details of notation.

4.5 Model 5

This model represents the interaction of N^c and E^c field with the messenger field E^c_m so consequently N^c and E^c get negative corrections at one-loop and positive two-loop corrections. The other fields interacting with them receive two-loop corrections, as given below

$$\begin{aligned}
\delta M^2_{\tilde{L}} &= \Big[-\frac{\alpha_\lambda\,(\alpha_N+\alpha_\tau)}{16\pi^2}\Big]\Lambda^2\\
\delta M^2_{\tilde{E}^c} &= \Big[-\frac{\alpha_\lambda}{24\pi}x^2h(x)+\frac{\alpha_\lambda\,(-12\alpha_1+10\alpha_N+15\alpha_\lambda)}{80\pi^2}\Big]\Lambda^2\\
\delta M^2_{\tilde{N}^c} &= \Big[-\frac{\alpha_\lambda}{24\pi}x^2h(x)+\frac{\alpha_\lambda\,(-12\alpha_1+15\alpha_\lambda+10\alpha_\tau)}{80\pi^2}\Big]\Lambda^2\\
\delta M^2_{H_u} &= \Big[-\frac{\alpha_N\alpha_\lambda}{16\pi^2}\Big]\Lambda^2\\
\delta M^2_{H_d} &= \Big[-\frac{\alpha_\lambda\alpha_\tau}{16\pi^2}\Big]\Lambda^2\\
\delta A_\tau &= \Big[-\frac{\alpha_\lambda}{4\pi}\Big]\Lambda\\
\delta A_N &= \Big[-\frac{\alpha_\lambda}{4\pi}\Big]\Lambda.
\end{aligned}\tag{4.8}$$

As can be seen from the above, Eq. (4.8), this model leaves the stop sector including A_t untouched. The variation of the lightest sparticles eigenvalues with λ are presented in Fig. 5(a). As can be seen from the figure, for $x = 0.5$, the cancellations are really strong

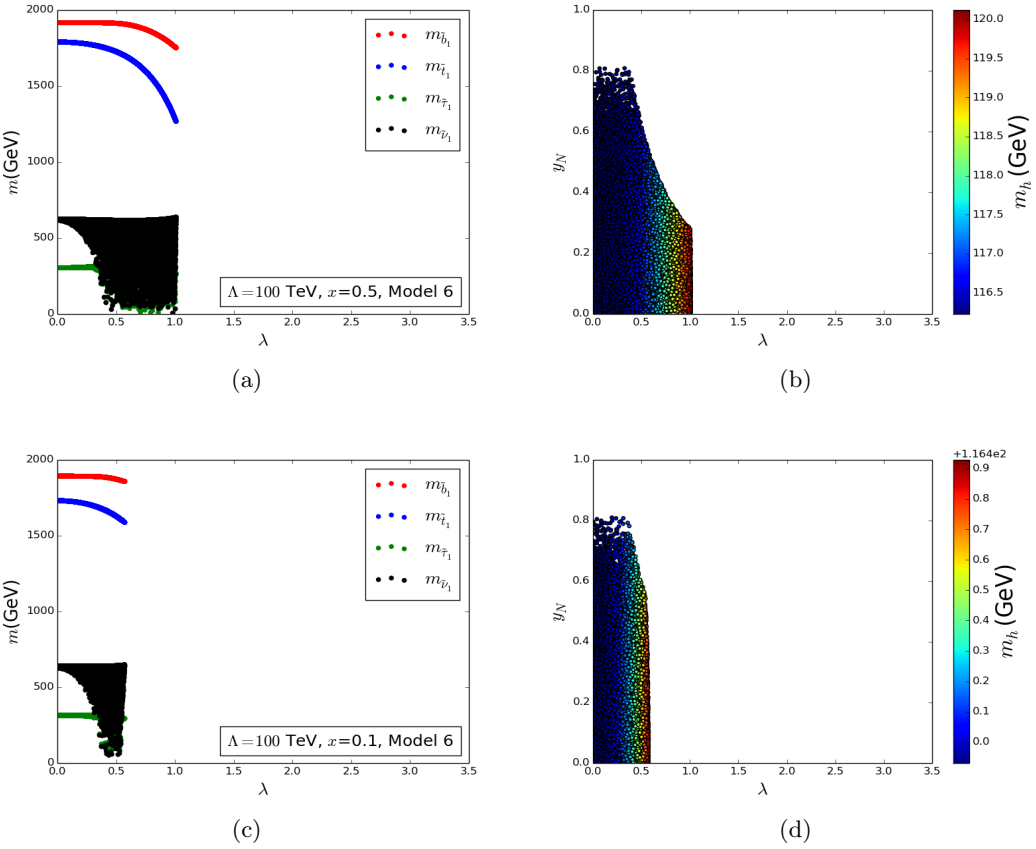

Figure 6. Model 6: Spectrum variation with λ and Higgs mass values in y_N and λ plane. Please see caption of Fig. 1 for details of notation.

and there are two distinct regions of λ which are viable phenomenologically: $\lambda \lesssim 0.2$ and $1.7 \lesssim \lambda \lesssim 2.25$. For lower values of the λ, the stau becomes tachyonic as the one-loop contributions from matter messenger mixing lead to significant cancellations in the boundary conditions. For larger values of $\lambda \gtrsim 2.0$, the A_τ becomes large leading again to tachyonic spectrum of the $\tilde{\tau}$. The region with $\lambda \lesssim 0.2$ is irrelevant phenomenologically and thus not pursued further. From Fig. 5(c) we see that the cancellations are extremely mild and almost disappear for $x = 0.1$. For $\lambda \gtrsim 1.5$, the spectrum turns tachyonic and thus unphysical.

The Higgs mass values are shown in Figs. 5(b) and 5(d) for $x = 0.5$ and $x = 0.1$ respectively. Unlike in Models 1 and 2, A_N does not have a factor three in its messenger-matter contributions, Eq.(4.8). Since sleptons are not heavy so this model is also not able to produce correct Higgs mass.

In Table 6, the spectra for four benchmark points are shown. It can be seen that for all the points, Higgs mass is 116 GeV as A_N is not sufficiently large and sleptons are light.

Parameter	x = 0.5	x = 0.5	x = 0.1	x = 0.1	Parameter	x = 0.5	x = 0.5	x = 0.1	x = 0.1
λ	2.00	1.79	1.46	1.02	y_N	0.40	0.45	0.47	0.28
A_N	−2491.1	−1974.5	−1303.8	−683.0	A_t	−569.4	−569.3	−685.0	−698.0
m_R	5960.8	5980.6	6631.0	4818.2	μ	848.	836.	884.	765.
$m_{\tilde{\nu}_1}$	271.	260.	435.	611.	$m_{\tilde{\nu}_{2,3}}/m_{\nu_{2,3}}$	5961.	5981.	6632.	4818.
m_h	116.11	116.64	116.04	116.15	m_H	1052.	1038.	1096.	1004.
$m_h^{0+\Delta}$	116.08	116.60	116.03	116.14	m_{A^0}	1066.	1052.	1108.	1005.
m_h^0	115.84	115.84	115.94	115.95	$m_{H^\pm}$	1068.	1055.	1110.	1008.
M_S	1851.	1847.	1806.	1797.	$m_{\tilde{g}}$	2188.	2188.	2112.	2111.
$\tilde{t}_1$	1804.	1798.	1747.	1735.	$\tilde{t}_2$	1901.	1897.	1867.	1861.
$\tilde{b}_1$	1913.	1916.	1888.	1892.	$\tilde{b}_2$	1917.	1920.	1893.	1898.
$\tilde{\tau}_1$	221.	262.	216.	300.	$\tilde{\tau}_2$	221.	285.	216.	300.
$\tilde{u}_1$	1936.	1931.	1916.	1909.	$\tilde{u}_2$	1969.	1970.	1940.	1940.
$\tilde{d}_1$	1917.	1920.	1894.	1898.	$\tilde{d}_2$	1955.	1956.	1923.	1923.
$\tilde{e}_1$	275.	285.	438.	612.	$\tilde{e}_2$	647.	634.	665.	648.
N_1	431.	430.	412.	411.	N_2	779.	774.	764.	720.
N_3	854.	842.	890.	770.	N_4	904.	898.	920.	845.
C_1	768.	763.	751.	711.	C_2	892.	886.	910.	832.

Table 6. Benchmark points for Model 5. See caption of Table 2 for details of notation.

4.6 Model 6

This model represents the interaction $W_{\rm mix} = \lambda N^c H_u H_d^m$. This is also a Type II model. One-loop and two-loop corrections at the boundary are given below:

$$\begin{aligned}
\delta M^2_{\tilde{Q}} &= \Big[-\frac{3\alpha_t\alpha_\lambda}{16\pi^2}\Big]\Lambda^2 \\
\delta M^2_{\tilde{U}^c} &= \Big[-\frac{3\alpha_t\alpha_\lambda}{8\pi^2}\Big]\Lambda^2 \\
\delta M^2_{\tilde{L}} &= \Big[-\frac{9\alpha_N\alpha_\lambda}{16\pi^2}\Big]\Lambda^2 \\
\delta M^2_{H_u} &= \Big[-\frac{\alpha_\lambda}{8\pi}x^2h(x) + \frac{3\alpha_\lambda\left(-3\alpha_1 - 15\alpha_2 + 10\left(\alpha_N + 5\alpha_\lambda\right)\right)}{80\pi^2}\Big]\Lambda^2 \\
\delta M^2_{\tilde{N}^c} &= \Big[-\frac{\alpha_\lambda}{4\pi}x^2h(x) + \frac{3\alpha_\lambda\left(5\left(-3\alpha_2 + 2\alpha_N + 3\alpha_t + 10\alpha_\lambda\right) - 3\alpha_1\right)}{40\pi^2}\Big]\Lambda^2 \\
\delta A_t &= \Big[-\frac{3\alpha_\lambda}{4\pi}\Big]\Lambda \\
\delta A_N &= \Big[-\frac{9\alpha_\lambda}{4\pi}\Big]\Lambda.
\end{aligned} \tag{4.9}$$

In this model, two-loop messenger-matter contributions to $\tilde{Q}, \tilde{U}^c$ and $\tilde{L}$ masses are negative whereas $\delta M^2_{H_u}$ gets both negative and positive contribution. For $x = 0.5$ case the maximum allowed value for λ is ~ 1.0 as shown in Fig. 6(a). In Fig. 6(b), Higgs mass values are shown in the λ vs y_N plane. One can not achieve correct Higgs mass in this model.

For $x = 0.1$, one-loop effect is small and thus $M^2_{H_u}$ becomes more massive for increasing

Parameter	x = 0.5	x = 0.5	x = 0.1	x = 0.1	Parameter	x = 0.5	x = 0.5	x = 0.1	x = 0.1
λ	0.89	0.53	0.54	0.30	y_N	0.28	0.54	0.48	0.21
A_N	−4301.5	−1496.9	−1563.2	−524.4	A_t	−1768.2	−992.2	−1100.1	−828.1
m_R	3925.9	6678.3	9942.6	7868.5	μ	1395.	1510.	249.	781.
$m_{\tilde{\nu}_1}$	297.	257.	333.	629.	$m_{\tilde{\nu}_{2,3}}/m_{\nu_{2,3}}$	3927.	6679.	9943.	7869.
m_h	118.93	116.84	117.10	116.53	m_H	1535.	1629.	666.	1016.
$m_h^{0+\Delta}$	118.92	116.80	117.08	116.53	m_{A^0}	1543.	1649.	676.	1018.
m_h^0	116.23	116.22	116.33	116.33	$m_{H^\pm}$	1545.	1651.	681.	1020.
M_S	1643.	1803.	1724.	1778.	$m_{\tilde{g}}$	2181.	2186.	2108.	2111.
$\tilde{t}_1$	1462.	1715.	1604.	1701.	$\tilde{t}_2$	1846.	1896.	1853.	1859.
$\tilde{b}_1$	1821.	1910.	1863.	1891.	$\tilde{b}_2$	1925.	1925.	1897.	1900.
$\tilde{\tau}_1$	259.	233.	289.	313.	$\tilde{\tau}_2$	301.	320.	293.	316.
$\tilde{u}_1$	1928.	1930.	1908.	1908.	$\tilde{u}_2$	1942.	1948.	1914.	1930.
$\tilde{d}_1$	1933.	1925.	1902.	1900.	$\tilde{d}_2$	1934.	1933.	1902.	1911.
$\tilde{e}_1$	301.	320.	293.	316.	$\tilde{e}_2$	341.	341.	338.	631.
N_1	431.	431.	236.	411.	N_2	823.	821.	253.	729.
N_3	1403.	1518.	422.	787.	N_4	1408.	1523.	807.	853.
C_1	805.	807.	243.	719.	C_2	1399.	1512.	790.	840.

Table 7. Benchmark points for Model 6. See caption of Table 2 for details of notation.

λ. But we cannot consider very large λ value because above certain value electro-weak symmetry breaking (EWSB) will be impossible. The allowed value of λ for successful EWSB is $\lesssim 0.6$ as shown in Fig. 6(c). As allowed values of λ are small, A_N is not very large, consequently one can not get correct Higgs mass.

In Table 7, we show four benchmark points, two for $x = 0.5$ and two for $x = 0.1$. Here A_t is less than A_N. Only for the first benchmark point, Higgs mass is raised by 2 GeV (from MSSM contribution) and others have small A_N, so there is no correction at all.

4.7 Model 7

This model is a Type II model. Here messenger-matter interaction superpotential is $W_{\rm mix} = \lambda N^c H_d H_u^m$. Non-zero corrections to the different soft parameters are shown in Eq. (4.10). $\delta M^2_{H_d}$ and $\delta M^2_{\tilde{N}^c}$ get both negative one-loop and positive two-loop corrections and other

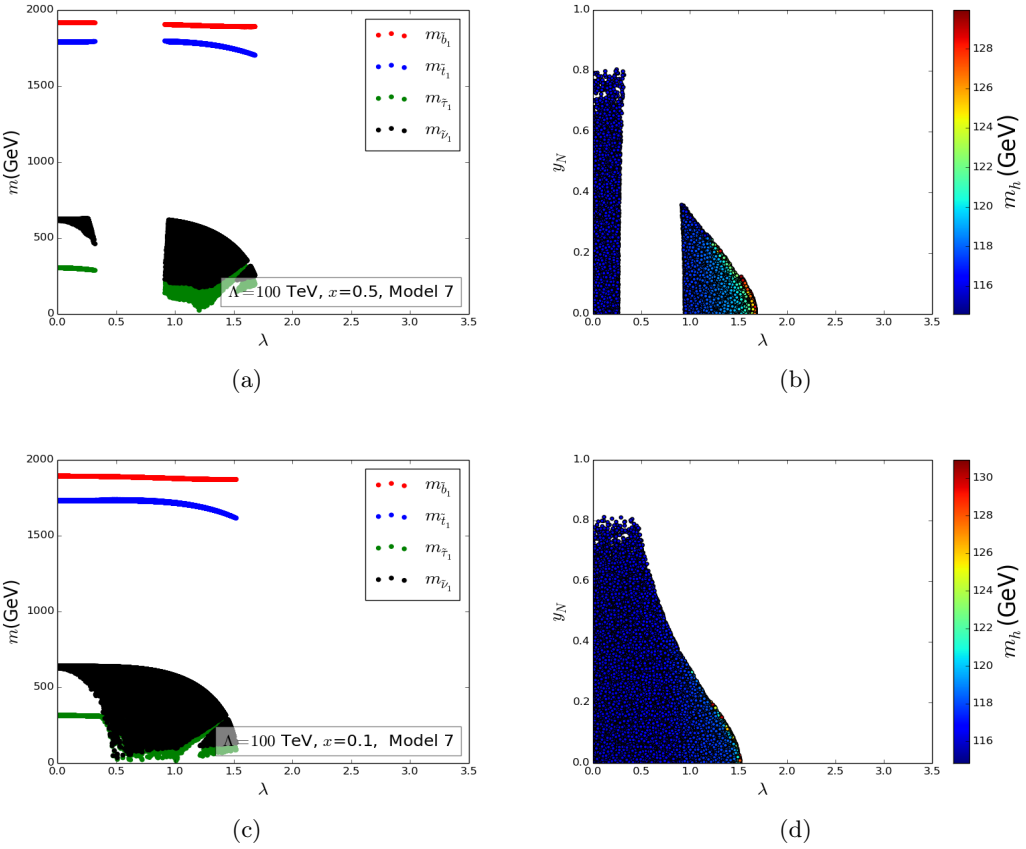

Figure 7. Model 7: Spectrum variation with λ and Higgs mass values in y_N and λ plane. Please see caption of Fig. 1 for details of notation.

soft masses gets two-loop negative corrections only.

$$
\begin{aligned}
\delta M^2_{\tilde{Q}} &= \Big[-\frac{3\alpha_b\alpha_\lambda}{16\pi^2}\Big]\Lambda^2 \\
\delta M^2_{\tilde{D}^c} &= \Big[-\frac{3\alpha_b\alpha_\lambda}{8\pi^2}\Big]\Lambda^2 \\
\delta M^2_{\tilde{L}} &= \Big[-\frac{3\alpha_\lambda\left(2\alpha_N+\alpha_\tau\right)}{16\pi^2}\Big]\Lambda^2 \\
\delta M^2_{\tilde{E}^c} &= \Big[-\frac{3\alpha_\lambda\alpha_\tau}{8\pi^2}\Big]\Lambda^2 \\
\delta M^2_{H_u} &= \Big[-\frac{3\alpha_N\alpha_\lambda}{8\pi^2}\Big]\Lambda^2 \\
\delta M^2_{H_d} &= \Big[-\frac{\alpha_\lambda}{8\pi}x^2h(x) + \frac{3\alpha_\lambda\left(-3\alpha_1-15\alpha_2+10\left(\alpha_N+5\alpha_\lambda\right)\right)}{80\pi^2}\Big]\Lambda^2 \\
\delta M^2_{\tilde{N}^c} &= \Big[-\frac{\alpha_\lambda}{4\pi}x^2h(x) + \frac{3\alpha_\lambda\left(5\left(-3\alpha_2+3\alpha_b+10\alpha_\lambda+\alpha_\tau\right)-3\alpha_1\right)}{40\pi^2}\Big]\Lambda^2 \\
\delta A_b &= \Big[-\frac{3\alpha_\lambda}{4\pi}\Big]\Lambda \\
\delta A_\tau &= \Big[-\frac{3\alpha_\lambda}{4\pi}\Big]\Lambda \\
\delta A_N &= \Big[-\frac{3\alpha_\lambda}{2\pi}\Big]\Lambda.
\end{aligned}
\tag{4.10}
$$

Parameter	x = 0.5	x = 0.5	x = 0.1	x = 0.1	Parameter	x = 0.5	x = 0.5	x = 0.1	x = 0.1
λ	1.60	1.34	1.26	1.43	y_N	0.07	0.17	0.17	0.09
A_N	−9785.4	−6806.3	−5988.2	−7756.1	A_t	−583.6	−574.8	−692.3	−698.4
m_R	6480.5	3029.5	7172.6	7859.8	μ	929.	858.	932.	957.
$m_{\tilde{\nu}_1}$	275.	281.	238.	164.	$m_{\tilde{\nu}_{2,3}}/m_{\nu_{2,3}}$	6481.	3030.	7173.	7860.
m_h	125.73	120.38	118.71	123.27	m_H	7172.	4394.	5315.	6890.
$m_h^{0+\Delta}$	125.73	120.47	118.71	123.27	m_{A^0}	7165.	4392.	5316.	6885.
m_h^0	116.23	116.23	116.33	116.33	$m_{H^\pm}$	7165.	4393.	5317.	6885.
M_S	1779.	1821.	1752.	1717.	$m_{\tilde{g}}$	2187.	2187.	2111.	2110.
$\tilde{t}_1$	1723.	1769.	1685.	1646.	$\tilde{t}_2$	1838.	1875.	1821.	1791.
$\tilde{b}_1$	1891.	1894.	1873.	1870.	$\tilde{b}_2$	1933.	1922.	1906.	1914.
$\tilde{\tau}_1$	210.	201.	202.	112.	$\tilde{\tau}_2$	448.	462.	522.	414.
$\tilde{u}_1$	1862.	1905.	1858.	1822.	$\tilde{u}_2$	1968.	1966.	1941.	1942.
$\tilde{d}_1$	1957.	1934.	1925.	1943.	$\tilde{d}_2$	2005.	1980.	1967.	1988.
$\tilde{e}_1$	448.	485.	522.	414.	$\tilde{e}_2$	625.	485.	568.	690.
N_1	430.	430.	411.	411.	N_2	804.	785.	774.	777.
N_3	938.	866.	942.	967.	N_4	967.	913.	964.	987.
C_1	790.	773.	760.	763.	C_2	955.	901.	953.	976.

Table 8. Benchmark points for Model 7. See caption of Table 2 for details of notation.

There is no constraint on H_d mass from tachyonic mass condition. Thus one may expect large λ here. For both the value of x, maximum allowed values of λ is ~ 1.5 because beyond this point lightest stau becomes tachyonic. However, there exists two band of λ values for $x = 0.5$ because of "non-convergent Higgs spectrum" as can be seen in Fig. 7(a). One gets a 125 GeV Higgs (Fig. 7(b)& (d)) for $\lambda \sim 1.5$ in both cases.

In this model A_t term is not generated at the boundary. A_N is responsible for generation of correct Higgs mass. One can see from the benchmark points in Table 8 that absolute values of A_N can be ~ 10 TeV for $x = 0.5$. Typical correction to the Higgs mass from its MSSM value (m_h^0) is 8 GeV. In all the benchmark points, $A_t(M_{\rm SUSY})$ is always less than A_N.

4.8 Model 8

This is a Type II model having $W_{mix} = \frac{1}{2}\lambda N^c N^c S^m$. Note that S_m is a gauge singlet. Thus if we consider the messenger sector to be consists of only this field then no usual soft masses will be generated. That is why we consider two sets of messengers: (a) singlet (S_m), which appears in the $W_{\rm mix}$ and $5 \oplus \bar{5}$, which gives usual GMSB boundary conditions. None of the MSSM fields get one-loop corrections here. However they get two-loop negative corrections as shown in the equation below. The field $\tilde{N}^c$ gets both the one-loop and

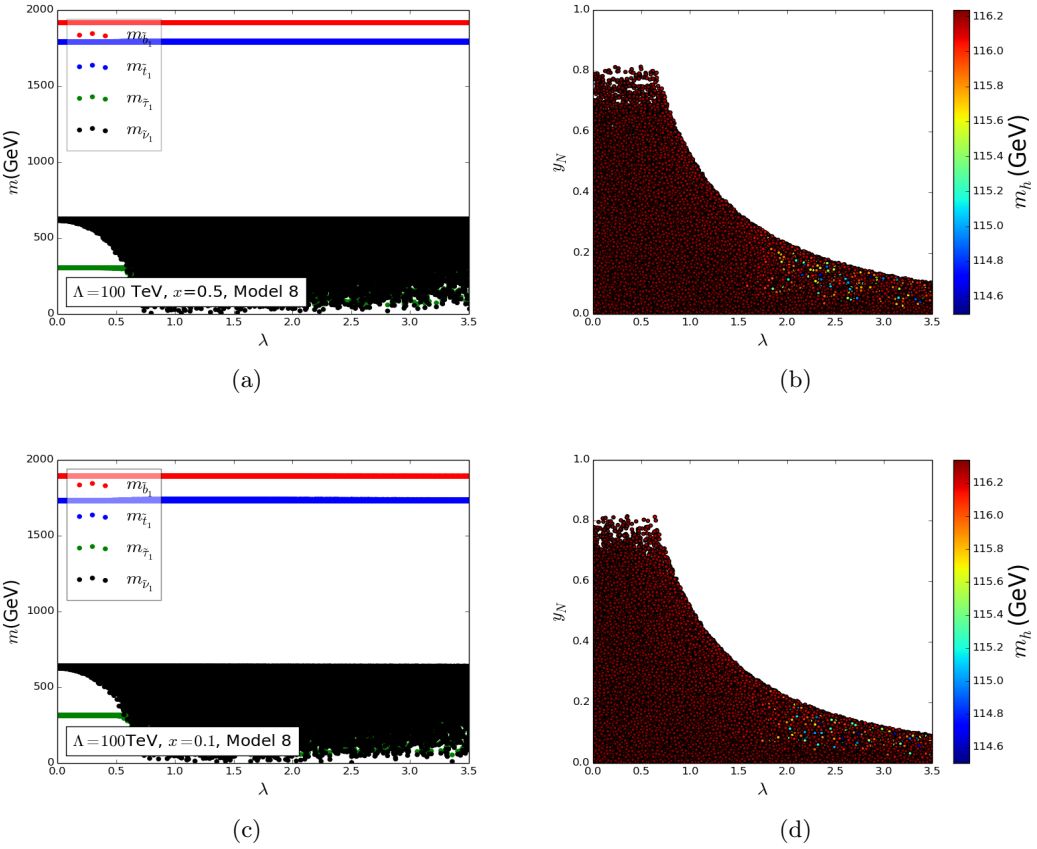

Figure 8. Model 8: Spectrum variation with λ and Higgs mass values in y_N and λ plane. Please see caption of Fig. 1 for details of notation.

two-loop corrections.

$$\begin{aligned}
\delta M^2_{\tilde{L}} &= \Big[-\frac{3\alpha_N\alpha_\lambda}{16\pi^2}\Big]\Lambda^2 \\
\delta M^2_{H_u} &= \Big[-\frac{3\alpha_N\alpha_\lambda}{16\pi^2}\Big]\Lambda^2 \\
\delta M^2_{\tilde{N}^c} &= \Big[-\frac{\alpha_\lambda}{8\pi}x^2 h(x) + \frac{3\alpha_\lambda\left(4\alpha_N+13\alpha_\lambda\right)}{32\pi^2}\Big]\Lambda^2 \\
\delta A_N &= \Big[-\frac{3\alpha_\lambda}{4\pi}\Big]\Lambda. \qquad (4.11)
\end{aligned}$$

As $\delta M^2_{\tilde{L}}$ is negative, $d_{1,2}$ will not be small enough to raise the Higgs mass. That is why we are not getting a 125 GeV Higgs even though very large values of λ are allowed (Fig. 8(a) & (c)) and ~ 10 TeV A_N is generated the $M_{\rm SUSY}$ scale (Table 9).

In this model no other A-terms except the A_N is generated at the boundary. As we have discussed earlier only A_N is not sufficient. One also need direct coupling of $\tilde{L}$ with the messenger field to get correct Higgs mass.

Parameter	x = 0.5	x = 0.5	x = 0.1	x = 0.1	Parameter	x = 0.5	x = 0.5	x = 0.1	x = 0.1
λ	2.53	0.98	2.79	1.52	y_N	0.12	0.37	0.12	0.29
A_N	-12137.9	-1814.3	-14733.5	-4307.4	A_t	-576.05	-575.24	-689.4	-682.4
m_R	2374.2	5253.4	4854.8	7984.7	μ	800.	762.	926.	921.
$m_{\tilde{\nu}_1}$	367.	456.	261.	272.	$m_{\tilde{\nu}_{2,3}}/m_{\nu_{2,3}}$	2377.	5254.	4855.	7985.
m_h	115.47	116.20	116.23	116.27	m_H	1028.	989.	1131.	1114.
$m_h^{0+\Delta}$	116.21	116.19	116.27	116.25	m_{A^0}	1026.	995.	1136.	1132.
m_h^0	116.23	116.22	116.33	116.33	$m_{H^\pm}$	1029.	998.	1138.	1135.
M_S	1843.	1843.	1798.	1799.	$m_{\tilde{g}}$	2188.	2188.	2111.	2111.
$\tilde{t}_1$	1793.	1793.	1738.	1739.	$\tilde{t}_2$	1894.	1894.	1861.	1861.
$\tilde{b}_1$	1917.	1917.	1892.	1892.	$\tilde{b}_2$	1921.	1921.	1898.	1898.
$\tilde{\tau}_1$	299.	302.	256.	261.	$\tilde{\tau}_2$	306.	306.	318.	318.
$\tilde{u}_1$	1929.	1929.	1907.	1907.	$\tilde{u}_2$	1969.	1969.	1942.	1942.
$\tilde{d}_1$	1921.	1921.	1899.	1898.	$\tilde{d}_2$	1955.	1955.	1926.	1926.
$\tilde{e}_1$	306.	306.	318.	318.	$\tilde{e}_2$	390.	461.	330.	330.
N_1	430.	430.	412.	412.	N_2	755.	730.	771.	770.
N_3	806.	767.	932.	928.	N_4	880.	867.	956.	952.
C_1	746.	721.	757.	757.	C_2	867.	853.	946.	942.

Table 9. Benchmark points for Model 8. See caption of Table 2 for details of notation.

4.9 Model 9

This model is based on the $W_{mix} = \lambda N^c S S_m$ interaction. Like the previous model, messenger sector consists of two types of fields for the same reasons: (a) singlet (S_m), which appears in the $W_{\rm mix}$ and $5 \oplus \bar{5}$, which gives usual GMSB boundary conditions. Soft mass corrections from $W_{\rm mix}$ are given below:

$$\begin{aligned}
\delta M^2_{\tilde{L}} &= \Big[-\frac{3\alpha_N\alpha_\lambda}{16\pi^2}\Big]\Lambda^2 \\
\delta M^2_{H_u} &= \Big[-\frac{3\alpha_N\alpha_\lambda}{16\pi^2}\Big]\Lambda^2 \\
\delta M^2_{\tilde{N}^c} &= \Big[-\frac{\alpha_\lambda}{8\pi}x^2 h(x) + \frac{21\alpha_\lambda^2}{16\pi^2}\Big]\Lambda^2 \\
\delta M^2_{\tilde{S}} &= \Big[-\frac{\alpha_\lambda}{8\pi}x^2 h(x) + \frac{3\alpha_\lambda\,(2\alpha_N + 7\alpha_\lambda)}{16\pi^2}\Big]\Lambda^2 \\
\delta A_N &= \Big[-\frac{3\alpha_\lambda}{4\pi}\Big]\Lambda. \qquad (4.12)
\end{aligned}$$

Here $\delta M^2_{\tilde{S}}$ has both the one-loop and two-loop contributions. Note that SUSY preserving mass of $\tilde{S}$ is μ_s which is too small. Secondly, $\tilde{S}$ do not get any mass from gauge mediation as it is SM gauge singlet. Thus lower values of λ are ruled out by requirement

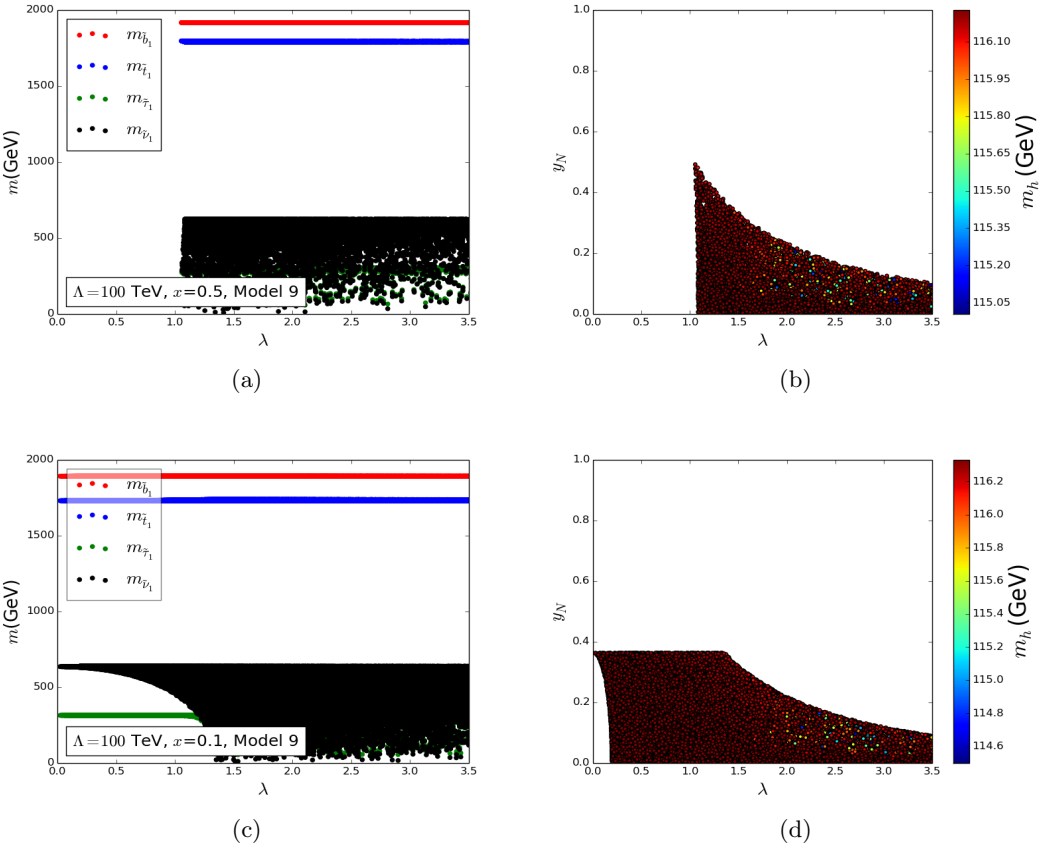

Figure 9. Model 9: Spectrum variation with λ and Higgs mass values in y_N and λ plane. Please see caption of Fig. 1 for details of notation.

of non-negative soft mass of $\tilde{S}$:

$$\lambda \geq \sqrt{\left(\frac{2}{3}x^2 h(x)\pi - 2\alpha_N\right)\frac{4}{7}\pi}. \tag{4.13}$$

Another point to be noted that $\delta M_{\tilde{S}}^2$ is RG invariant below the messenger scale as there is no Yukawa or trilinear coupling involving $\tilde{S}$ below that.

Spectrum of this model is similar to the previous model except for the fact that λ has now lower limit as shown in Fig. 9(a) and Fig. 9(c). These values are ~ 1 and ~ 0.2 for $x = 0.5$ and $x = 0.1$ respectively. The squark masses are independent of λ as can be seen in Fig. 9(a) and Fig. 9(c).

Higgs mass values are given in λ vs y_N plane. Note that we are getting Higgs mass around 116 GeV. Failure of this depicts the importance of heavy slepton. In this model, sleptons are not heavy as they are not getting any messenger-matter correction. Hence $d_{1,2}$ are large and there is no significant increase in the Higgs mass. In this model also only A_N is generated at the boundary. In Table 10, four benchmark points are shown.

Parameter	x = 0.5	x = 0.5	x = 0.1	x = 0.1	Parameter	x = 0.5	x = 0.5	x = 0.1	x = 0.1
λ	2.40	1.49	2.26	1.08	y_N	0.10	0.22	0.17	0.36
A_N	−10950.2	−4218.6	−9702.2	−2178.6	A_t	−580.8	−575.3	−684.6	−684.3
m_R	5772.3	3053.2	3746.7	4631.7	μ	732.	763.	939.	872.
$m_{\tilde{\nu}_1}$	508.	452.	195.	418.	$m_{\tilde{\nu}_{2,3}}/m_{\nu_{2,3}}$	5772.	3054.	3748.	4632.
m_h	116.21	116.17	116.10	116.29	m_H	968.	996.	1144.	1085.
$m_h^{0+\Delta}$	116.21	116.19	116.25	116.27	m_{A^0}	972.	996.	1147.	1091.
m_h^0	116.23	116.23	116.33	116.33	$m_{H^\pm}$	975.	999.	1149.	1094.
M_S	1842.	1843.	1799.	1798.	$m_{\tilde{g}}$	2188.	2188.	2111.	2111.
$\tilde{t}_1$	1792.	1793.	1739.	1737.	$\tilde{t}_2$	1894.	1894.	1861.	1861.
$\tilde{b}_1$	1917.	1917.	1892.	1892.	$\tilde{b}_2$	1921.	1921.	1898.	1898.
$\tilde{\tau}_1$	303.	302.	202.	311.	$\tilde{\tau}_2$	306.	306.	318.	318.
$\tilde{u}_1$	1929.	1929.	1907.	1907.	$\tilde{u}_2$	1969.	1969.	1942.	1941.
$\tilde{d}_1$	1921.	1921.	1898.	1899.	$\tilde{d}_2$	1954.	1955.	1926.	1925.
$\tilde{e}_1$	306.	306.	318.	318.	$\tilde{e}_2$	512.	459.	324.	425.
N_1	429.	430.	412.	412.	N_2	707.	731.	772.	761.
N_3	737.	768.	945.	878.	N_4	860.	868.	967.	911.
C_1	699.	722.	759.	749.	C_2	845.	853.	958.	901.

Table 10. Benchmark points for Model 9. See caption of Table 2 for details of notation.

4.10 Model 10

This is a Type I model with $W_{mix} = \lambda N^c H_u^m H_d^m$. Note that, in this interaction there is only one matter field. Thus choices of the messenger fields are arbitrary. For example, one can have (a) $N^c 1_m \bar{1}_m$, (b) $N^c 5_m \bar{5}_m$, and (c) $N^c 10_m \overline{10}_m$. Here we consider the messenger having representation $5 \oplus \bar{5}$. The corrections to the soft masses for this messenger-matter interaction at the boundary are given in Eq. (4.14). The $\delta M^2_{\tilde{N}^c}$ gets both one-loop negative and two-loop positive corrections. The $\delta M^2_{\tilde{L}}$ and $\delta M^2_{H_u}$ are generated at two-loop level.

$$\begin{aligned}
\delta M^2_{\tilde{L}} &= \Big[-\frac{3\alpha_N\alpha_\lambda}{8\pi^2} \Big]\Lambda^2 \\
\delta M^2_{H_u} &= \Big[-\frac{3\alpha_N\alpha_\lambda}{8\pi^2} \Big]\Lambda^2 \\
\delta M^2_{\tilde{N}^c} &= \Big[-\frac{\alpha_\lambda}{2\pi} x^2 h(x) + \frac{3\alpha_\lambda\left(-3\alpha_1 - 15\alpha_2 + 40\alpha_\lambda\right)}{40\pi^2} \Big]\Lambda^2 \\
\delta A_N &= \Big[-\frac{3\alpha_\lambda}{2\pi} \Big]\Lambda. \qquad (4.14)
\end{aligned}$$

Spectral variation with λ of this model is similar to models 8 and 9 which is expected from the nature of messenger-matter corrections: (a) all of them get corrections to $M^2_{\tilde{L}}, M^2_{\tilde{N}^c}, M^2_{H_u}$ and A_N, and (b) right handed neutrinos are much heavier compared to the messenger-matter corrections at the boundary. Though λ can be very large (Fig. 10(a) & (c)) and a very large A_N is generated at the $M_{\rm SUSY}$ scale (Table 11), Higgs mass obtained can be atmost 117 GeV (Fig. 10(b) & (d)). This model also fails like the previous two models for

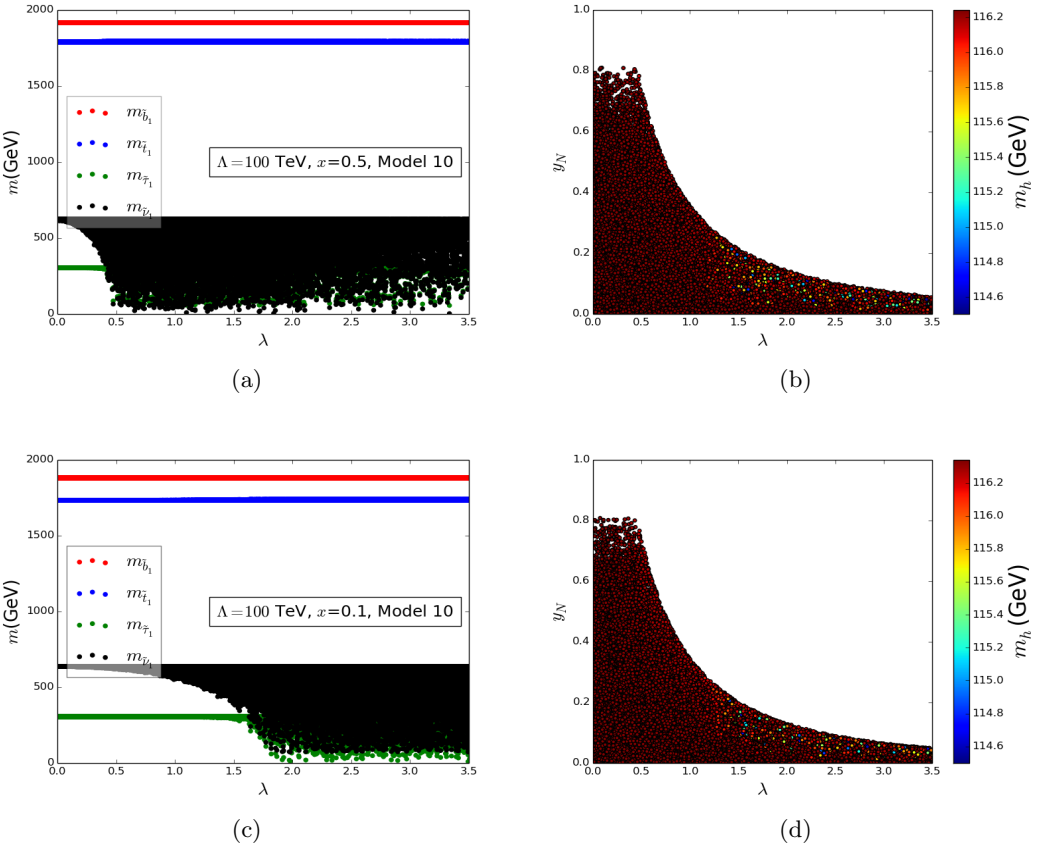

Figure 10. Model 10: Spectrum variation with λ and Higgs mass values in y_N and λ plane. Please see caption of Fig. 1 for details of notation.

the same reason. The benchmark points are given in Table 11.

4.11 Model 11

This is a Type II model with the messenger-matter interaction term $W_{\rm mix} = \lambda LQD_m$. Here messenger fields belong to $5 \oplus \bar{5}$ representation. As both the matter fields are SU(2) doublets, all the MSSM fields get corrections to their soft masses as well as non-zero trilinear couplings.

$$\delta M^2_{\tilde{Q}} = \Big[-\frac{\alpha_\lambda}{8\pi} x^2 h(x) + \frac{\alpha_\lambda \left(5\left(-9\alpha_2 - 16\alpha_3 + 3\left(\alpha_N + 14\alpha_\lambda + \alpha_\tau\right)\right) - 7\alpha_1\right)}{80\pi^2} \Big] \Lambda^2$$

$$\delta M^2_{\tilde{U}^c} = \Big[-\frac{3\alpha_t \alpha_\lambda}{8\pi^2} \Big] \Lambda^2$$

$$\delta M^2_{\tilde{D}^c} = \Big[-\frac{3\alpha_b \alpha_\lambda}{8\pi^2} \Big] \Lambda^2$$

$$\delta M^2_{\tilde{L}} = \Big[-3\frac{\alpha_\lambda}{8\pi} x^2 h(x) + \frac{3\alpha_\lambda \left(5\left(-9\alpha_2 - 16\alpha_3 + 3\left(\alpha_b + \alpha_t + 14\alpha_\lambda\right)\right) - 7\alpha_1\right)}{80\pi^2} \Big] \Lambda^2$$

Parameter	x = 0.5	x = 0.5	x = 0.1	x = 0.1	Parameter	x = 0.5	x = 0.5	x = 0.1	x = 0.1
λ	2.28	0.99	2.25	1.04	y_N	0.10	0.36	0.10	0.27
A_N	-19775.1	-3696.8	-19295.2	-4050.9	A_t	-575.6	-568.4	-690.3	-684.8
m_R	3577.1	8253.0	6582.5	5477.0	μ	861.	873.	945.	889.
$m_{\tilde{\nu}_1}$	164.	81.	169.	374.	$m_{\tilde{\nu}_{2,3}}/m_{\nu_{2,3}}$	3579.	8253.	6583.	5477.
m_h	115.56	116.09	116.24	116.28	m_H	1074.	1062.	1144.	1096.
$m_h^{0+\Delta}$	116.17	116.07	116.26	116.27	m_{A^0}	1076.	1086.	1153.	1105.
m_h^0	116.23	116.23	116.33	116.33	$m_{H^\pm}$	1079.	1089.	1155.	1108.
M_S	1844.	1845.	1798.	1798.	$m_{\tilde{g}}$	2188.	2188.	2111.	2111.
$\tilde{t}_1$	1795.	1796.	1738.	1737.	$\tilde{t}_2$	1894.	1895.	1861.	1861.
$\tilde{b}_1$	1917.	1917.	1892.	1892.	$\tilde{b}_2$	1921.	1921.	1898.	1898.
$\tilde{\tau}_1$	186.	81.	170.	308.	$\tilde{\tau}_2$	306.	306.	318.	318.
$\tilde{u}_1$	1929.	1929.	1907.	1907.	$\tilde{u}_2$	1970.	1970.	1942.	1942.
$\tilde{d}_1$	1921.	1921.	1898.	1899.	$\tilde{d}_2$	1956.	1957.	1926.	1925.
$\tilde{e}_1$	306.	306.	318.	318.	$\tilde{e}_2$	312.	310.	323.	386.
N_1	430.	431.	412.	412.	N_2	784.	788.	773.	765.
N_3	867.	879.	952.	896.	N_4	913.	921.	973.	925.
C_1	772.	776.	760.	752.	C_2	901.	909.	964.	915.

Table 11. Benchmark points for Model 10. See caption of Table 2 for details of notation.

$$
\begin{aligned}
\delta M^2_{\tilde{E}^c} &= \Big[-\frac{9\alpha_\lambda\alpha_\tau}{8\pi^2}\Big]\Lambda^2 \\
\delta M^2_{H_u} &= \Big[-\frac{9\left(\alpha_N+\alpha_t\right)\alpha_\lambda}{16\pi^2}\Big]\Lambda^2 \\
\delta M^2_{H_d} &= \Big[-\frac{9\alpha_\lambda\left(\alpha_b+\alpha_\tau\right)}{16\pi^2}\Big]\Lambda^2 \\
\delta M^2_{\tilde{N}^c} &= \Big[-\frac{9\alpha_N\alpha_\lambda}{8\pi^2}\Big]\Lambda^2 \\
\delta A_t &= \Big[-\frac{3\alpha_\lambda}{4\pi}\Big]\Lambda \\
\delta A_b &= \Big[-\frac{3\alpha_\lambda}{4\pi}\Big]\Lambda \\
\delta A_\tau &= \Big[-\frac{9\alpha_\lambda}{4\pi}\Big]\Lambda \\
\delta A_N &= \Big[-\frac{9\alpha_\lambda}{4\pi}\Big]\Lambda. \qquad (4.15)
\end{aligned}
$$

Here $\delta M^2_{\tilde{L}}$ gets one-loop negative and two-loop positive contributions. For $x = 0.5$, one-loop contribution dominates over two-loop contributions in this model. For very small value of $\lambda(\gtrsim 0.1)$, lightest stau and sneutrino become tachyonic as shown in Fig. 11(a) and again become positive for $\lambda > 1$. On the other hand, for $x = 0.1$, two-loop negative contribution to $M^2_{\tilde{E}^c}$ is responsible for smallness of λ. Here lightest stau and sneutrino become tachyonic for $\lambda \gtrsim 0.15$ and large λ region (0.6-1.1) provides positive spectrum. In this model, all the A-terms are generated at the boundary. We can see from the (Fig. 11(b) and Fig. 11(d),

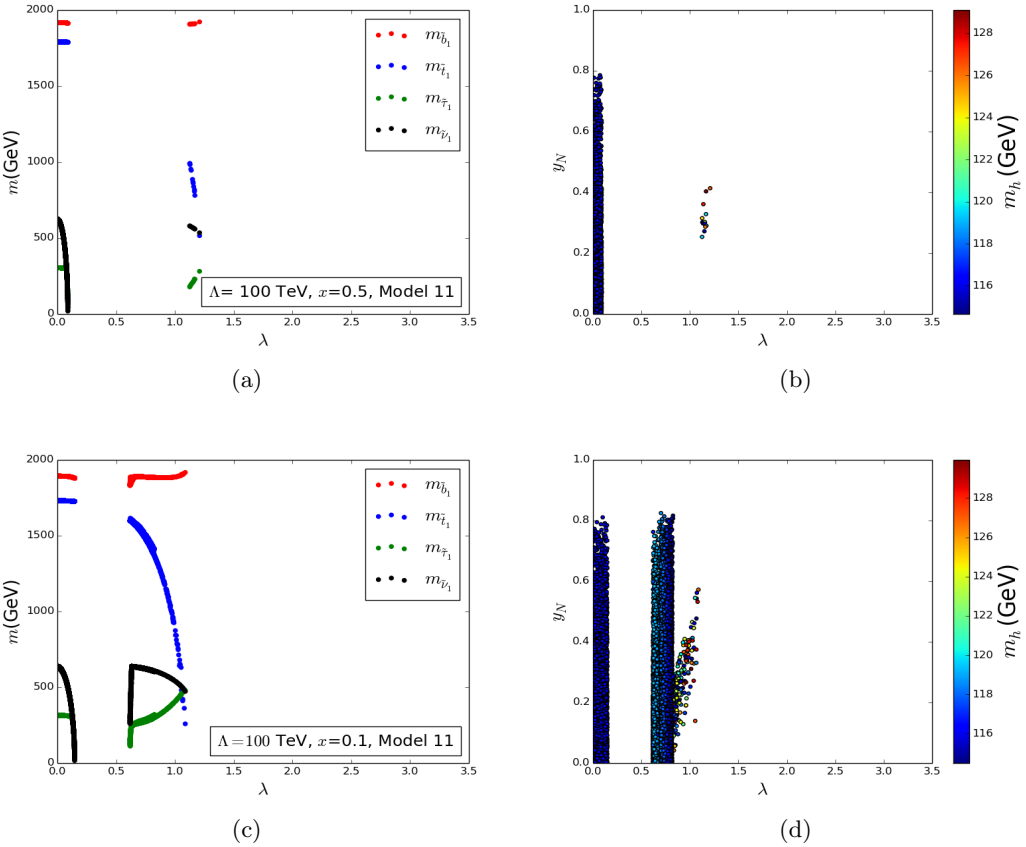

Figure 11. Model 11: Spectrum variation with λ and Higgs mass values in y_N and λ plane. Please see caption of Fig. 1 for details of notations.

the upper allowed band of λ in both $x = 0.5$ and $x = 0.1$ case can provide correct Higgs mass. In Table 12, four benchmark points for this models are shown. One can see from Table 12 that the combination of both matter-messenger and neutrino-sneutrino corrections will reproduce correct Higgs mass and one may get tachyonic spectrum including only the matter-messenger boundary conditions.

4.12 Model 12

This model represents the messenger-matter interaction superpotential $W_{\rm mix} = \lambda L D^c Q_m$. Here messenger fields transform as $10 \oplus \overline{10}$. One-loop and two-loop corrections due to this

Parameter	x = 0.5	x = 0.5	x = 0.1	x = 0.1	Parameter	x = 0.5	x = 0.5	x = 0.1	x = 0.1
λ	1.16	1.13	0.81	0.74	y_N	0.29	0.32	0.11	0.14
A_N	−7366.9	−6930.3	−3616.7	−3008.0	A_t	−2601.8	−2484.2	−1624.7	−1472.0
m_R	5154.4	4568.6	3015.6	2158.0	μ	2157.	2095.	1465.	1331.
$m_{\tilde{\nu}_1}$	4947.	4290.	2982.	2113.	$m_{\tilde{\nu}_{2,3}}/m_{\nu_{2,3}}$	5161.	4576.	3022.	2169.
m_h	126.14	124.72	125.66	122.15	m_H	2153.	2105.	1576.	1463.
$m_h^{0+\Delta}$	−−	−−	114.25	117.34	m_{A^0}	2200.	2148.	1579.	1464.
m_h^0	116.23	116.23	116.33	116.33	$m_{H^\pm}$	2197.	2146.	1580.	1466.
M_S	1264.	1376.	1613.	1673.	$m_{\tilde{g}}$	2203.	2200.	2117.	2114.
$\tilde{t}_1$	838.	991.	1390.	1491.	$\tilde{t}_2$	1908.	1909.	1872.	1876.
$\tilde{b}_1$	1909.	1907.	1885.	1888.	$\tilde{b}_2$	1943.	1936.	1903.	1902.
$\tilde{\tau}_1$	217.	182.	294.	272.	$\tilde{\tau}_2$	4958.	4300.	2993.	2131.
$\tilde{u}_1$	1916.	1918.	1895.	1903.	$\tilde{u}_2$	2027.	2022.	1996.	1997.
$\tilde{d}_1$	1943.	1937.	1903.	1903.	$\tilde{d}_2$	2028.	2024.	1997.	1999.
$\tilde{e}_1$	477.	441.	402.	361.	$\tilde{e}_2$	570.	584.	617.	630.
N_1	431.	431.	412.	412.	N_2	834.	832.	788.	787.
N_3	2148.	2087.	1473.	1339.	N_4	2150.	2090.	1478.	1345.
C_1	807.	807.	770.	770.	C_2	2156.	2095.	1468.	1335.

Table 12. Benchmark points for Model 11. See caption of Table 2 for details of notation.

interaction are shown below:

$$
\begin{aligned}
\delta M^2_{\tilde{Q}} &= \Big[-\frac{\alpha_b\alpha_\lambda}{8\pi^2}\Big]\Lambda^2 \\
\delta M^2_{\tilde{D}^c} &= \Big[-\frac{\alpha_\lambda}{12\pi}x^2h(x) + \frac{\alpha_\lambda\left(-7\alpha_1+5\left(-9\alpha_2-16\alpha_3+3\alpha_N+18\alpha_\lambda+3\alpha_\tau\right)\right)}{120\pi^2}\Big]\Lambda^2 \\
\delta M^2_{\tilde{L}} &= \Big[-\frac{\alpha_\lambda}{8\pi}x^2h(x) + \frac{\alpha_\lambda\left(-7\alpha_1-45\alpha_2-80\alpha_3+30\alpha_b+90\alpha_\lambda\right)}{80\pi^2}\Big]\Lambda^2 \\
\delta M^2_{\tilde{E}^c} &= \Big[-\frac{3\alpha_\lambda\alpha_\tau}{8\pi^2}\Big]\Lambda^2 \\
\delta M^2_{\tilde{N}^c} &= \Big[-\frac{3\alpha_N\alpha_\lambda}{8\pi^2}\Big]\Lambda^2 \\
\delta M^2_{H_u} &= \Big[-\frac{3\alpha_N\alpha_\lambda}{16\pi^2}\Big]\Lambda^2 \\
\delta M^2_{H_d} &= \Big[-\frac{3\alpha_\lambda\left(2\alpha_b+\alpha_\tau\right)}{16\pi^2}\Big]\Lambda^2 \\
\delta A_b &= \Big[-\frac{\alpha_\lambda}{2\pi}\Big]\Lambda \\
\delta A_\tau &= \Big[-\frac{3\alpha_\lambda}{4\pi}\Big]\Lambda \\
\delta A_N &= \Big[-\frac{3\alpha_\lambda}{4\pi}\Big]\Lambda.
\end{aligned}
\tag{4.16}
$$

Here $\delta M^2_{\tilde{D}^c}$ and $\delta M^2_{\tilde{L}}$ get both the one-loop negative and two-loop positive contributions. For $x = 0.5$, cancellation between one-loop and two-loop contribution to $M^2_{\tilde{L}}$ is severe. We

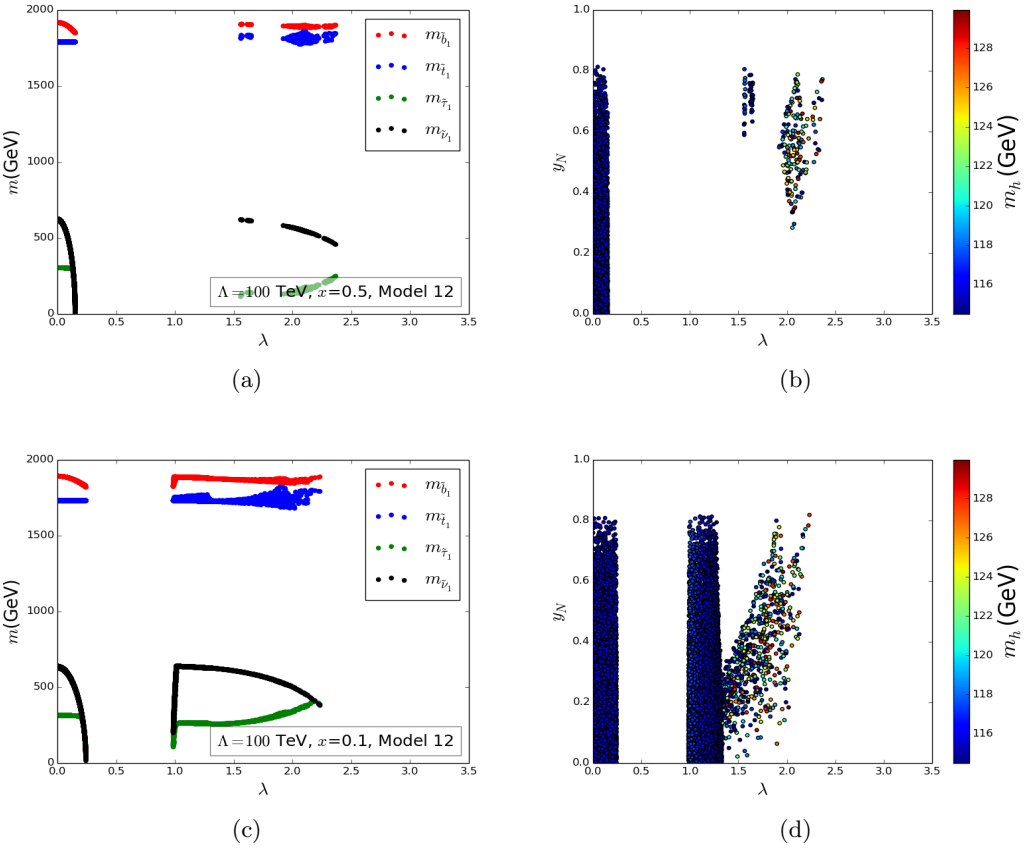

Figure 12. Model 12: Spectrum variation with λ and Higgs mass values in y_N and λ plane. Please see caption of Fig. 1 for details of notation.

can see from Fig. 12(a) and Fig. 12(c), two band of λ values are allowed in both $x = 0.5$ and $x = 0.1$ case.

Here all the A-terms, except A_t, are generated. In larger λ region, we can achieve a 125 GeV Higgs. In the Table 13, four benchmark points are shown for this model. Like model 11, in this model also, for $x = 0.5$ case, only the combination of matter-messenger mixing and neutrino-sneutrino corrections can provide positive spectrum and one may get tachyonic spectrum considering only the matter messenger mixing boundary conditions.

Parameter	x = 0.5	x = 0.5	x = 0.1	x = 0.1	Parameter	x = 0.5	x = 0.5	x = 0.1	x = 0.1
λ	2.11	1.96	1.55	1.34	y_N	0.50	0.49	0.20	0.24
A_N	−8138.8	−7044.0	−4541.8	−3381.1	A_t	−501.2	−514.9	−686.7	−685.3
m_R	7297.3	7115.6	5011.5	3108.0	μ	1726.	1520.	854.	860.
$m_{\tilde{\nu}_1}$	8098.	6325.	4904.	3219.	$m_{\tilde{\nu}_{2,3}}/m_{\nu_{2,3}}$	7295.	7119.	5014.	3103.
m_h	124.62	124.33	125.54	124.33	m_H	1536.	1414.	952.	1009.
$m_h^{0+\Delta}$	−−	−−	109.21	113.62	m_{A^0}	1726.	1552.	964.	1017.
m_h^0	116.23	116.23	116.33	116.33	$m_{H^\pm}$	1719.	1548.	962.	1018.
M_S	1836.	1841.	1781.	1790.	$m_{\tilde{g}}$	2206.	2203.	2123.	2120.
$\tilde{t}_1$	1801.	1802.	1719.	1729.	$\tilde{t}_2$	1871.	1881.	1845.	1853.
$\tilde{b}_1$	1889.	1892.	1867.	1876.	$\tilde{b}_2$	1932.	1927.	1904.	1900.
$\tilde{\tau}_1$	158.	132.	265.	259.	$\tilde{\tau}_2$	8093.	6330.	4910.	3210.
$\tilde{u}_1$	1893.	1906.	1890.	1899.	$\tilde{u}_2$	1965.	1965.	1932.	1936.
$\tilde{d}_1$	1992.	1984.	1947.	1939.	$\tilde{d}_2$	2016.	2014.	1998.	1997.
$\tilde{e}_1$	520.	450.	431.	370.	$\tilde{e}_2$	550.	581.	609.	629.
N_1	432.	432.	412.	412.	N_2	824.	823.	759.	760.
N_3	1733.	1529.	860.	866.	N_4	1737.	1534.	898.	902.
C_1	805.	805.	744.	746.	C_2	1727.	1523.	886.	891.

Table 13. Benchmark points for Model 12. See caption of Table 2 for details of notation.

4.13 Model 13

Model 13 is Type II model having $W_{mix} = \lambda L E^c H_d^m$ and soft mass corrections are listed below :

$$\begin{aligned}
\delta M^2_{\tilde{L}} &= \Big[-\frac{\alpha_\lambda}{8\pi} x^2 h(x) + \frac{3\alpha_\lambda\left(-9\alpha_1 - 15\alpha_2 + 10\left(5\alpha_\lambda + \alpha_\tau\right)\right)}{80\pi^2}\Big]\Lambda^2 \\
\delta M^2_{\tilde{E}^c} &= \Big[-\frac{\alpha_\lambda}{4\pi} x^2 h(x) + \frac{3\alpha_\lambda\left(5\left(-3\alpha_2 + \alpha_N + 10\alpha_\lambda + 2\alpha_\tau\right) - 9\alpha_1\right)}{40\pi^2}\Big]\Lambda^2 \\
\delta M^2_{H_u} &= \Big[-\frac{3\alpha_N\alpha_\lambda}{16\pi^2}\Big]\Lambda^2 \\
\delta M^2_{H_d} &= \Big[-\frac{9\alpha_\lambda\alpha_\tau}{16\pi^2}\Big]\Lambda^2 \\
\delta M^2_{\tilde{N}^c} &= \Big[-\frac{3\alpha_N\alpha_\lambda}{8\pi^2}\Big]\Lambda^2 \\
\delta A_\tau &= \Big[-\frac{9\alpha_\lambda}{4\pi}\Big]\Lambda^2 \\
\delta A_N &= \Big[-\frac{3\alpha_\lambda}{4\pi}\Big]\Lambda. \qquad (4.17)
\end{aligned}$$

Here both $\delta M^2_{\tilde{L}}$ and $\delta M^2_{\tilde{E}^c}$ get one-loop negative correction and two-loop positive correction. As earlier, the interplay between the positive and negative contributions plays an important role. Parameter space for λ is broken down into two parts. In the region where λ is small, one-loop contributions dominate over the two-loop contributions. Just above $\lambda \sim 0.1$ (~ 0.2), lightest stau becomes tachyonic for $x = 0.5\,(0.1)$ as shown in Fig. 13(a) and

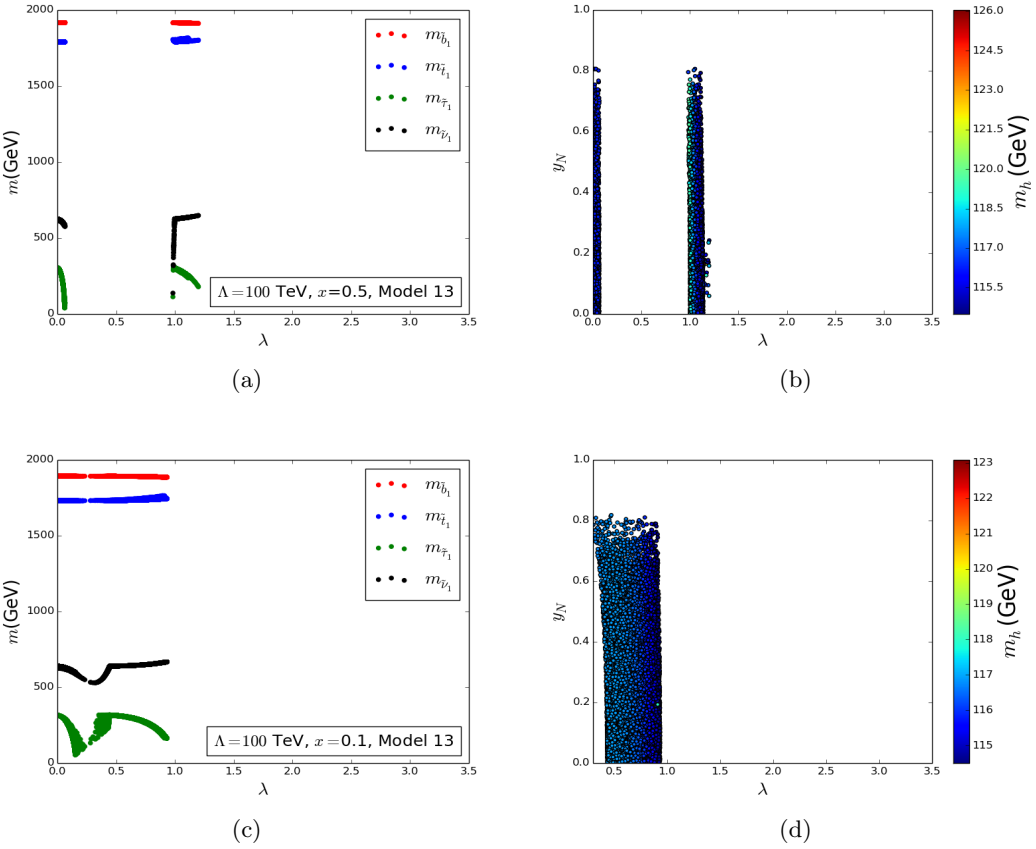

Figure 13. Model 13: Spectrum variation with λ and Higgs mass values in y_N and λ plane. Note that origins of two right panel plots are 1.0 and 0.3 respectively. Please see caption of Fig. 1 for details of notation.

Fig. 13(c). After certain values of λ, the two-loop contributions dominate over the one-loop contributions. Note that, the gap between two regions of parameter spaces of λ is larger for $x = 0.5$ which is expected. Higgs mass values are shown in Fig. 13(b) and Fig. 13(d). In the second region where λ is higher, a 125 GeV Higgs is achievable.

Here at the boundary, A_τ and A_N are generated. In Table 14, four benchmark points are shown for both x=0.5 and 0.1 case, the absolute values of A_N at the $M_{\rm SUSY}$ scale is $\gtrsim 1.5$ TeV. The Higgs mass is raised by 4-10 GeV in these points(Table 14).

4.14 Model 14

This model has the following messenger-matter interaction superpotential, $W_{\rm mix} = \lambda L H_d E^c_m$. The boundary conditions generated for this superpotential are shown in Eq. (4.18). All the scalar fields of MSSM except $\tilde{U}^c$ get these corrections. Both $\delta M^2_{\tilde{L}}$ and $\delta M^2_{H_d}$ get one-loop negative and the two-loop positive contributions. Rest of the fields get only two-loop

Parameter	x = 0.5	x = 0.5	x = 0.1	x = 0.1	Parameter	x = 0.5	x = 0.5	x = 0.1	x = 0.1
λ	1.14	0.99	0.82	0.89	y_N	0.17	0.57	0.10	0.05
A_N	−2493.9	−1808.9	−1294.8	−1517.2	A_t	−581.6	−564.2	−700.1	−700.7
m_R	2326.9	9630.6	2054.6	2437.1	μ	700.	915.	764.	763.
$m_{\tilde{\nu}_1}$	2284.	556.	2023.	2450.	$m_{\tilde{\nu}_{2,3}}/m_{\nu_{2,3}}$	2340.	9631.	2063.	2434.
m_h	126.02	119.55	123.18	119.50	m_H	911.	1066.	992.	991.
$m_h^{0+\Delta}$	113.72	119.5	115.46	114.98	m_{A^0}	914.	1104.	993.	992.
m_h^0	116.23	116.22	116.33	116.33	$m_{H^\pm}$	916.	1107.	996.	994.
M_S	1847.	1847.	1800.	1802.	$m_{\tilde{g}}$	2188.	2188.	2111.	2111.
$\tilde{t}_1$	1797.	1799.	1738.	1741.	$\tilde{t}_2$	1898.	1896.	1864.	1866.
$\tilde{b}_1$	1914.	1916.	1889.	1888.	$\tilde{b}_2$	1918.	1921.	1895.	1893.
$\tilde{\tau}_1$	2307.	300.	2051.	2439.	$\tilde{\tau}_2$	3163.	937.	2763.	3327.
$\tilde{u}_1$	1936.	1929.	1914.	1917.	$\tilde{u}_2$	1967.	1971.	1939.	1938.
$\tilde{d}_1$	1918.	1921.	1895.	1893.	$\tilde{d}_2$	1952.	1957.	1920.	1919.
$\tilde{e}_1$	644.	536.	659.	666.	$\tilde{e}_2$	644.	630.	659.	666.
N_1	430.	430.	412.	412.	N_2	681.	797.	720.	719.
N_3	705.	921.	769.	769.	N_4	856.	952.	845.	845.
C_1	673.	785.	710.	710.	C_2	839.	941.	831.	831.

Table 14. Benchmark points for Model 13. See caption of Table 2 for details of notation.

Parameter	x = 0.5	x = 0.5	x = 0.1	x = 0.1	Parameter	x = 0.5	x = 0.5	x = 0.1	x = 0.1
λ	2.16	1.82	2.16	1.59	y_N	0.30	0.18	0.37	0.17
A_N	−2926.0	−2108.4	−2875.0	−1624.1	A_t	−573.2	−581.1	−680.4	−697.9
m_R	3907.0	2220.9	5876.2	2981.9	μ	859.	693.	1077.	777.
$m_{\tilde{\nu}_1}$	4071.	2176.	5549.	2935.	$m_{\tilde{\nu}_{2,3}}/m_{\nu_{2,3}}$	3905.	2229.	5877.	2984.
m_h	125.39	120.65	124.87	120.93	m_H	4198.	2308.	5734.	3058.
$m_h^{0+\Delta}$	114.01	116.73	110.76	115.918	m_{A^0}	4202.	2308.	5740.	3058.
m_h^0	116.23	116.23	116.33	116.33	$m_{H^\pm}$	4202.	2310.	5740.	3059.
M_S	1803.	1831.	1692.	1767.	$m_{\tilde{g}}$	2188.	2188.	2111.	2111.
$\tilde{t}_1$	1750.	1779.	1623.	1702.	$\tilde{t}_2$	1858.	1884.	1763.	1836.
$\tilde{b}_1$	1908.	1905.	1900.	1887.	$\tilde{b}_2$	1934.	1922.	1938.	1907.
$\tilde{\tau}_1$	461.	295.	283.	451.	$\tilde{\tau}_2$	4064.	2192.	5553.	2941.
$\tilde{u}_1$	1884.	1917.	1789.	1876.	$\tilde{u}_2$	1971.	1966.	1957.	1941.
$\tilde{d}_1$	1945.	1928.	1958.	1915.	$\tilde{d}_2$	1983.	1966.	1993.	1945.
$\tilde{e}_1$	513.	406.	749.	528.	$\tilde{e}_2$	595.	600.	876.	569.
N_1	430.	429.	412.	411.	N_2	786.	676.	787.	729.
N_3	867.	699.	1088.	785.	N_4	915.	856.	1100.	854.
C_1	772.	668.	768.	718.	C_2	901.	839.	1089.	839.

Table 15. Benchmark points for Model 14. See caption of Table 2 for details of notation.

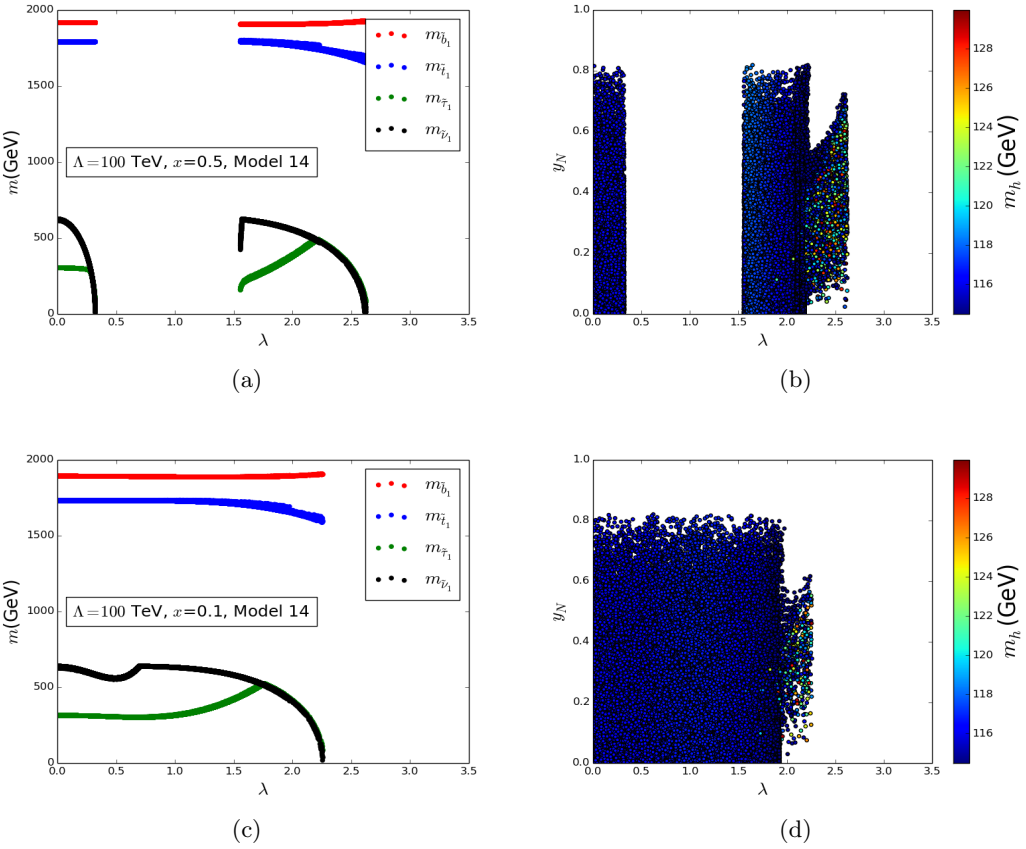

Figure 14. Model 14: Spectrum variation with λ and Higgs mass values in y_N and λ plane. Please see caption of Fig. 1 for details of notation.

negative corrections.

$$
\begin{aligned}
\delta M^2_{\tilde{Q}} &= \Big[-\frac{\alpha_b\alpha_\lambda}{16\pi^2}\Big]\Lambda^2 \\
\delta M^2_{\tilde{D}^c} &= \Big[-\frac{\alpha_b\alpha_\lambda}{8\pi^2}\Big]\Lambda^2 \\
\delta M^2_{\tilde{L}} &= \Big[-\frac{\alpha_\lambda}{24\pi}x^2h(x) + \frac{\alpha_\lambda\left(-9\alpha_1+5\left(-3\alpha_2+3\alpha_b+4\left(\alpha_\lambda+\alpha_\tau\right)\right)\right)}{80\pi^2}\Big]\Lambda^2 \\
\delta M^2_{\tilde{E}^c} &= \Big[-\frac{\alpha_\lambda\alpha_\tau}{4\pi^2}\Big]\Lambda^2 \\
\delta M^2_{\tilde{N}^c} &= \Big[-\frac{\alpha_N\alpha_\lambda}{8\pi^2}\Big]\Lambda^2 \\
\delta M^2_{H_u} &= \Big[-\frac{\alpha_N\alpha_\lambda}{16\pi^2}\Big]\Lambda^2 \\
\delta M^2_{H_d} &= \Big[-\frac{\alpha_\lambda}{24\pi}x^2h(x) + \frac{\alpha_\lambda\left(-9\alpha_1+5\left(-3\alpha_2+\alpha_N+4\left(\alpha_\lambda+\alpha_\tau\right)\right)\right)}{80\pi^2}\Big]\Lambda^2 \\
A_b &= \Big[-\frac{\alpha_\lambda}{4\pi}\Big]\Lambda \\
A_\tau &= \Big[-\frac{\alpha_\lambda}{2\pi}\Big]\Lambda \\
A_N &= \Big[-\frac{\alpha_\lambda}{4\pi}\Big]\Lambda.
\end{aligned}
\tag{4.18}
$$

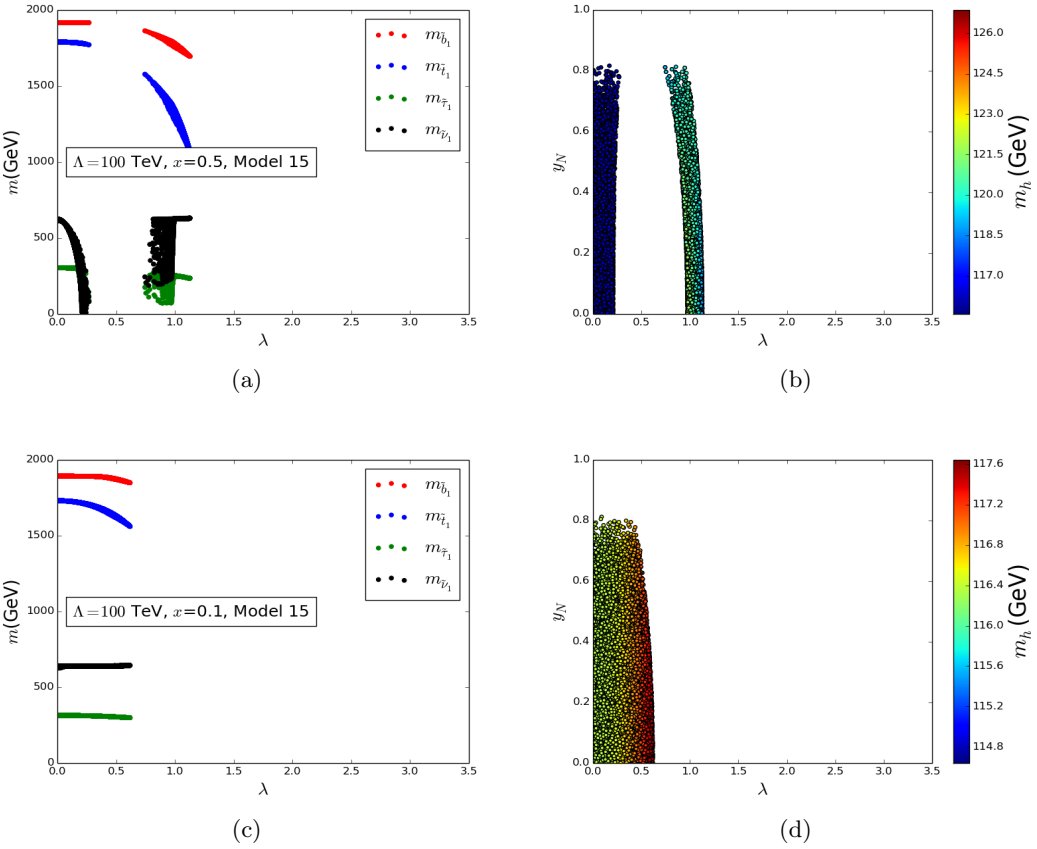

Figure 15. Model 15: Spectrum variation with λ and Higgs mass values in y_N and λ plane. Please see caption of Fig. 1 for details of notation.

We get two band of allowed values of λ for $x = 0.5$. Note that the one loop and two loop corrections are proportional to α_λ and α_λ^2 respectively. For the smaller values of λ, one-loop effect dominates over the two loop contribution and as a consequence lightest stau becomes tachyonic beyond $\lambda \sim 0.32$ as shown in Fig. 14(a). For larger values of λ, situation gets reversed. However, λ cannot be arbitrary large because otherwise $M_{H_d}^2$ will become very heavy and radiative electroweak symmetry breaking would not be possible. For the other case, where $x = 0.1$, one-loop effect is not so strong and the upper limit of λ is around ~ 2.3 (Fig. 14(c)).

In Fig. 14(b) and Fig. 14(d), Higgs mass values are shown in the λ vs y_N plane. For both the values of x, a 125 GeV Higgs is achievable. In Table 15 four benchmark points are shown. In this model, no A_t term is generated at the boundary. Therefore heavy sleptons ($\tilde{\tau}_2$) and A_N are responsible for giving correct Higgs mass.

4.15 Model 15

This is a Type II model based on $5 \oplus \bar{5}$ and S_m messenger fields like the model 8 and 9. The soft mass corrections based on the interaction $\lambda L H_u S_m$ are given by

$$\begin{aligned}
\delta M^2_{\tilde{Q}} &= \Big[-\frac{3\alpha_t\alpha_\lambda}{16\pi^2}\Big]\Lambda^2 \\
\delta M^2_{\tilde{U}^c} &= \Big[-\frac{3\alpha_t\alpha_\lambda}{8\pi^2}\Big]\Lambda^2 \\
\delta M^2_{\tilde{L}} &= \Big[-\frac{\alpha_\lambda}{8\pi}x^2 h(x) + \frac{3\alpha_\lambda\left(5\left(-3\alpha_2+4\alpha_N+3\alpha_t+8\alpha_\lambda\right)-3\alpha_1\right)}{80\pi^2}\Big]\Lambda^2 \\
\delta M^2_{\tilde{e}^c} &= \Big[-\frac{3\alpha_\lambda\alpha_\tau}{8\pi^2}\Big]\Lambda^2 \\
\delta M^2_{H_u} &= \Big[-\frac{\alpha_\lambda}{8\pi}x^2 h(x) + \frac{3\alpha_\lambda\left(5\left(-3\alpha_2+4\alpha_N+8\alpha_\lambda+\alpha_\tau\right)-3\alpha_1\right)}{80\pi^2}\Big]\Lambda^2 \\
\delta M^2_{H_d} &= \Big[-\frac{3\alpha_\lambda\alpha_\tau}{16\pi^2}\Big]\Lambda^2 \\
\delta M^2_{\tilde{N}^c} &= \Big[-\frac{3\alpha_N\alpha_\lambda}{4\pi^2}\Big]\Lambda^2 \\
\delta A_t &= \Big[-\frac{3\alpha_\lambda}{4\pi}\Big]\Lambda \\
\delta A_\tau &= \Big[-\frac{3\alpha_\lambda}{4\pi}\Big]\Lambda \\
\delta A_N &= \Big[-\frac{3\alpha_\lambda}{2\pi}\Big]\Lambda.
\end{aligned} \tag{4.19}$$

Here all the MSSM fields, except D^c, get these messenger-matter corrections. Both the $\delta M^2_{\tilde{L}}$ and $\delta M^2_{H_u}$ get one-loop and two-loop corrections. Like all the models where $\delta M^2_{\tilde{L}}$ gets one-loop negative contribution, this model is also a constrained model. One again, λ has two allowed regions for $x = 0.5$. Maximum value of λ in the first band is ~ 0.2 as shown in Fig. 15(a) and that value for the upper band is ~ 1.2 which is set by radiative electroweak breaking condition. For $x = 0.1$, there is only one band. The maximum value of λ is ~ 0.6 and this upper limit of λ is set by EWSB condition because $M^2_{H_u}$ gets positive correction whereas squarks get negative contributions at the boundary.

In the right panel on Fig. 15, Higgs mass values are shown. One cannot get correct Higgs mass for the case of $x = 0.1$ because λ is too small. In the other case, one can achieve it for the larger values of λ (Fig. 15(b)).

Four benchmark points of the model are shown in Table 16. In first benchmark point, we have 125 GeV Higgs mass. We see that a 10 GeV rise in the Higgs mass from the MSSM value.

4.16 Model 16

This is a Type II model with $W_{\rm mix} = \lambda L S H_u^m$. Corrections due to this superpotential to the soft mass are shown below. None of the squarks gets a correction. Both $\delta M^2_{\tilde{L}}$ and $\delta M^2_{\tilde{S}}$

Parameter	x = 0.5	x = 0.5	x = 0.1	x = 0.1	Parameter	x = 0.5	x = 0.5	x = 0.1	x = 0.1
λ	1.10	0.82	0.60	0.47	y_N	0.09	0.73	0.11	0.13
A_N	−4367.3	−2275.9	−1290.1	−802.4	A_t	−2429.9	−1561.6	−1206.5	−1012.3
m_R	1748.7	9648.0	2062.1	1640.4	μ	806.	1383.	326.	714.
$m_{\tilde{\nu}_1}$	1707.	468.	1284.	945.	$m_{\tilde{\nu}_{2,3}}/m_{\nu_{2,3}}$	1767.	9649.	2062.	1641.
m_h	126.01	119.80	117.47	117.05	m_H	1016.	1440.	706.	962.
$m_h^{0+\Delta}$	119.16	119.60	117.47	117.05	m_{A^0}	1018.	1529.	706.	962.
m_h^0	116.23	116.23	116.33	116.33	$m_{H^\pm}$	1020.	1531.	710.	965.
M_S	1416.	1683.	1706.	1749.	$m_{\tilde{g}}$	2178.	2182.	2107.	2109.
$\tilde{t}_1$	1144.	1521.	1576.	1647.	$\tilde{t}_2$	1752.	1863.	1848.	1857.
$\tilde{b}_1$	1716.	1842.	1854.	1880.	$\tilde{b}_2$	1928.	1925.	1899.	1900.
$\tilde{\tau}_1$	239.	252.	300.	306.	$\tilde{\tau}_2$	1729.	628.	1285.	947.
$\tilde{u}_1$	1942.	1927.	1903.	1910.	$\tilde{u}_2$	1955.	1939.	1913.	1916.
$\tilde{d}_1$	1948.	1931.	1904.	1902.	$\tilde{d}_2$	1948.	1932.	1904.	1902.
$\tilde{e}_1$	307.	306.	318.	318.	$\tilde{e}_2$	631.	485.	646.	644.
N_1	429.	431.	308.	410.	N_2	761.	822.	331.	685.
N_3	812.	1391.	426.	719.	N_4	887.	1396.	807.	829.
C_1	748.	805.	319.	677.	C_2	869.	1387.	790.	814.

Table 16. Benchmark points for Model 15. See caption of Table 2 for details of notation.

get negative one-loop and positive two-loop corrections.

$$\begin{aligned}
\delta M_{\tilde{L}}^2 &= \Big[-\frac{\alpha_\lambda}{8\pi} x^2 h(x) + \frac{3\alpha_\lambda \left(-3\alpha_1 - 15\alpha_2 + 50\alpha_\lambda\right)}{80\pi^2} \Big] \Lambda^2 \\
\delta M_{\tilde{e}^c}^2 &= \Big[-\frac{3\alpha_\lambda \alpha_\tau}{8\pi^2} \Big] \Lambda^2 \\
\delta M_{H_u}^2 &= \Big[-\frac{3\alpha_N \alpha_\lambda}{16\pi^2} \Big] \Lambda^2 \\
\delta M_{H_d}^2 &= \Big[-\frac{3\alpha_\lambda \alpha_\tau}{16\pi^2} \Big] \Lambda^2 \\
\delta M_{\tilde{N}^c}^2 &= \Big[-\frac{3\alpha_N \alpha_\lambda}{8\pi^2} \Big] \Lambda^2 \\
\delta M_{\tilde{S}}^2 &= \Big[-\frac{\alpha_\lambda}{4\pi} x^2 h(x) + \frac{3\alpha_\lambda \left(5\left(-3\alpha_2 + \alpha_N + 10\alpha_\lambda + \alpha_\tau\right) - 3\alpha_1\right)}{40\pi^2} \Big] \Lambda^2 \\
\delta A_\tau &= \Big[-\frac{3\alpha_\lambda}{4\pi} \Big] \Lambda \\
\delta A_N &= \Big[-\frac{3\alpha_\lambda}{4\pi} \Big] \Lambda.
\end{aligned} \tag{4.20}$$

Like the model 9, lower values of λ of this model are also ruled out by requirement of non-zero soft mass of $\tilde{S}$:

$$\lambda \geq \sqrt{\left(\frac{10}{3} x^2 h(x) \pi + 3\alpha_1 + 15\alpha_2 - 5\alpha_N - 5\alpha_\tau \right) \frac{2\pi}{25}}, \tag{4.21}$$

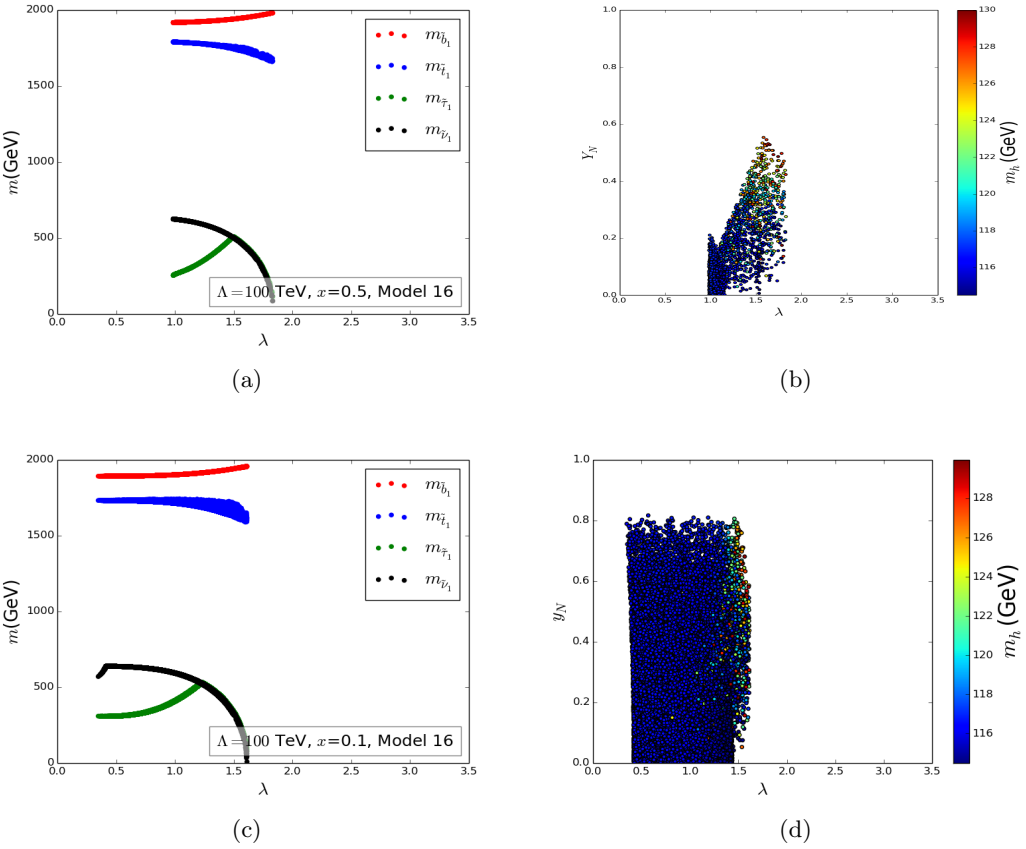

Figure 16. Model 16: Spectrum variation with λ and Higgs mass values in y_N and λ plane. Please see caption of Fig. 1 for details of notation.

where minimum value of λ has to be ~ 0.34 and 0.98 for $x = 0.1$ and $x = 0.5$ respectively. The sparticle eigenvalues are shown in Fig. 16(a) and Fig. 16(c).

Like other models, in Table 17, benchmark points, both for $x = 0.5$ and $x = 0.1$ case, are shown. We can see from this table and Fig. 16(b) and Fig. 16(d) that required Higgs mass can be achieved in this model. There is a 8 GeV increase in the Higgs mass from its pure MSSM values for all the benchmark points. We can see that all the points have heavy sleptons ($\tilde{\tau}_2$).

Parameter	x = 0.5	x = 0.5	x = 0.1	x = 0.1	Parameter	x = 0.5	x = 0.5	x = 0.1	x = 0.1
λ	1.47	1.25	1.48	0.96	y_N	0.34	0.24	0.25	0.23
A_N	−4031.4	−2944.9	−4153.3	−1767.2	A_t	−567.3	−577.7	−690.6	−695.7
m_R	5683.3	3311.6	7557.4	3021.5	μ	907.	727.	838.	776.
$m_{\tilde{\nu}_1}$	5544.	3368.	7325.	2955.	$m_{\tilde{\nu}_{2,3}}/m_{\nu_{2,3}}$	5687.	3305.	7558.	3024.
m_h	125.86	124.33	125.30	124.08	m_H	1012.	924.	880.	978.
$m_h^{0+\Delta}$	114.07	115.72	113.15	115.98	m_{A^0}	1042.	931.	902.	981.
m_h^0	116.23	116.23	116.33	116.33	$m_{H^\pm}$	1041.	932.	899.	984.
M_S	1809.	1829.	1706.	1782.	$m_{\tilde{g}}$	2188.	2188.	2111.	2111.
$\tilde{t}_1$	1757.	1778.	1636.	1718.	$\tilde{t}_2$	1862.	1883.	1778.	1848.
$\tilde{b}_1$	1938.	1925.	1939.	1900.	$\tilde{b}_2$	1943.	1929.	1950.	1907.
$\tilde{\tau}_1$	488.	354.	358.	392.	$\tilde{\tau}_2$	5547.	3362.	7327.	2964.
$\tilde{u}_1$	1887.	1914.	1806.	1892.	$\tilde{u}_2$	1979.	1971.	1963.	1943.
$\tilde{d}_1$	1943.	1929.	1950.	1907.	$\tilde{d}_2$	1969.	1958.	1957.	1928.
$\tilde{e}_1$	522.	425.	723.	437.	$\tilde{e}_2$	580.	593.	820.	607.
N_1	430.	429.	411.	411.	N_2	798.	704.	756.	727.
N_3	913.	732.	843.	782.	N_4	947.	861.	887.	851.
C_1	782.	695.	740.	716.	C_2	935.	843.	874.	837.

Table 17. Benchmark points for Model 16. See caption of Table 2 for details of notation.

4.17 Model 17

This model belongs to Type I category having interaction superpotential, $\lambda L H_u^m S^m$. The one-loop and two-loop corrections are given below :

$$\begin{aligned}
\delta M_{\tilde{L}}^2 &= \Big[-\frac{\alpha_\lambda}{4\pi} x^2 h(x) + \frac{9\alpha_\lambda\left(-\alpha_1 - 5\alpha_2 + 10\alpha_\lambda\right)}{80\pi^2} \Big] \Lambda^2 \\
\delta M_{\tilde{e^c}}^2 &= \Big[-\frac{3\alpha_\lambda \alpha_\tau}{8\pi^2} \Big] \Lambda^2 \\
\delta M_{H_u}^2 &= \Big[-\frac{3\alpha_N \alpha_\lambda}{16\pi^2} \Big] \Lambda^2 \\
\delta M_{H_d}^2 &= \Big[-\frac{3\alpha_\lambda \alpha_\tau}{16\pi^2} \Big] \Lambda^2 \\
\delta M_{\tilde{N}^c}^2 &= \Big[-\frac{3\alpha_N \alpha_\lambda}{8\pi^2} \Big] \Lambda^2 \\
\delta A_\tau &= \Big[-\frac{3\alpha_\lambda}{4\pi} \Big] \Lambda \\
\delta A_N &= \Big[-\frac{3\alpha_\lambda}{4\pi} \Big] \Lambda.
\end{aligned} \tag{4.22}$$

Because of one-loop negative contribution to $\delta M_{\tilde{L}}^2$, lightest stau and sneutrino become tachyonic beyond $\lambda \sim 0.12$ for the case of $x = 0.5$ as shown in Fig. 17(a). However for larger values of λ, two loop corrections overtake the one loop corrections and that is why we get the upper band of allowed values of λ. Correct Higgs mass is achievable for $\lambda \sim 2.0$ (see Fig. 17(b)). For $x = 0.1$, there is only one band of parameter space allowed for λ and

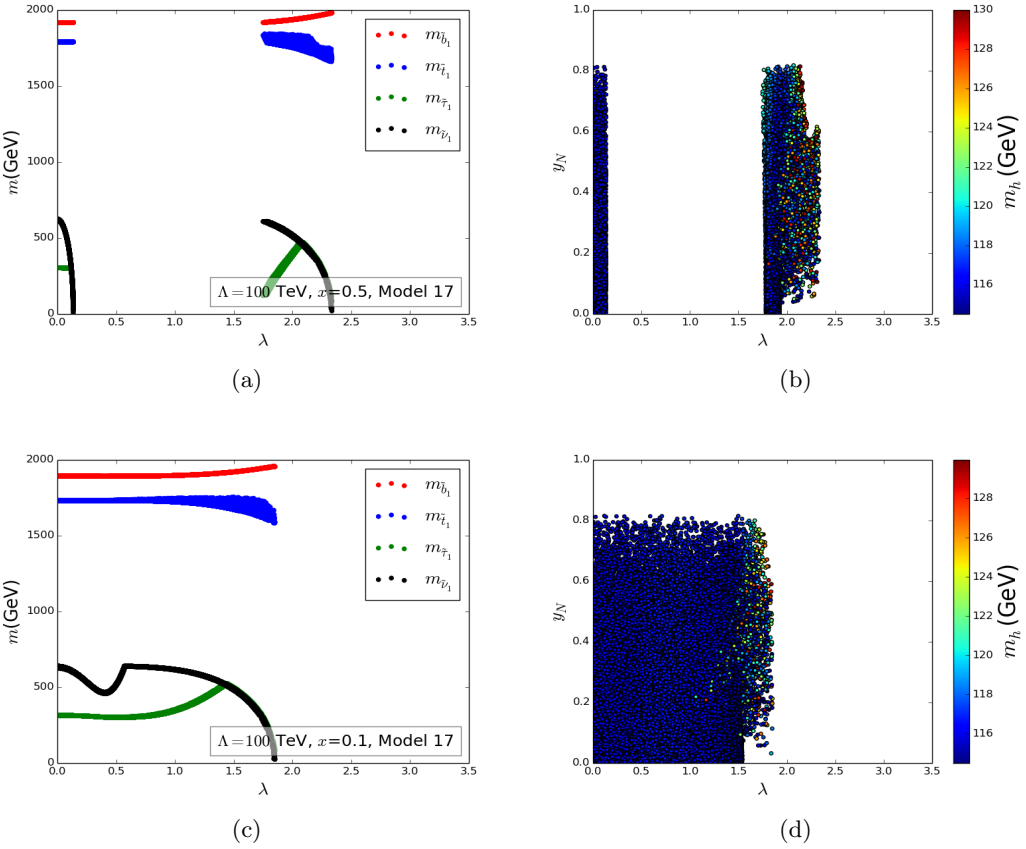

Figure 17. Model 17: Spectrum variation with λ and Higgs mass data points in y_N and λ plane. Please see caption of Fig. 1 for details of notation.

maximum allowed value of λ is ~ 1.8 as shown in Fig. 17(c). We have a parameter space near $\lambda \gtrsim 1.5$ and $y_N \gtrsim 0.2$ where we can achieve 125 GeV Higgs mass (Fig. 17(d)).

Four benchmark points for this model are shown in Table 18. In the second benchmark point, $M_{\tilde{L}}^2 - m_{\tilde{R}}^2$ is slightly large, so the contribution to the Higgs mass is less as compare to other benchmark points.

5 Discussion and conclusions

Gauge mediated supersymmetry breaking models are interesting due to their flavour blindness and unique phenomenological features like gravitino LSP etc. The discovery of the Higgs particle and the non-discovery of the coloured supersymmetric partners at the LHC has however put strong constraints on Gauge Mediated Supersymmetry Breaking models with vanishing A-terms, *i.e,* both minimal and general forms of them.

Allowing for direct matter-messenger interactions in addition to the standard gauge interactions is being pursued as one of the interesting solutions which allows for a light spectrum $\sim$ 1 TeV and a light CP even Higgs boson at 125 GeV. Several studies have been presented using these ideas, which culminated in survey Refs. [1, 2]. In the present

Parameter	x = 0.5	x = 0.5	x = 0.1	x = 0.1	Parameter	x = 0.5	x = 0.5	x = 0.1	x = 0.1
λ	2.02	1.81	1.43	1.02	y_N	0.23	0.28	0.39	0.18
A_N	−7680.1	−6180.1	−3781.2	−1984.2	A_t	−569.7	−562.9	−667.4	−697.2
m_R	5380.8	3372.8	5507.2	2412.2	μ	869.	918.	1086.	762.
$m_{\tilde{\nu}_1}$	5663.	2752.	5054.	2371.	$m_{\tilde{\nu}_{2,3}}/m_{\nu_{2,3}}$	5378.	3377.	5509.	2419.
m_h	124.50	119.16	124.46	124.61	m_H	957.	1067.	1164.	976.
$m_h^{0+\Delta}$	111.62	116.60	114.22	116.17	m_{A^0}	983.	1080.	1200.	978.
m_h^0	116.23	116.23	116.33	116.33	$m_{H^\pm}$	974.	1079.	1200.	981.
M_S	1806.	1837.	1762.	1786.	$m_{\tilde{g}}$	2188.	2188.	2112.	2111.
$\tilde{t}_1$	1754.	1788.	1700.	1723.	$\tilde{t}_2$	1860.	1888.	1826.	1852.
$\tilde{b}_1$	1939.	1922.	1916.	1898.	$\tilde{b}_2$	1944.	1927.	1923.	1904.
$\tilde{\tau}_1$	399.	180.	523.	349.	$\tilde{\tau}_2$	5659.	2758.	5058.	2388.
$\tilde{u}_1$	1885.	1918.	1858.	1897.	$\tilde{u}_2$	1979.	1972.	1954.	1942.
$\tilde{d}_1$	1944.	1927.	1923.	1904.	$\tilde{d}_2$	1969.	1960.	1944.	1926.
$\tilde{e}_1$	517.	393.	524.	397.	$\tilde{e}_2$	589.	603.	614.	621.
N_1	430.	431.	412.	411.	N_2	788.	799.	783.	719.
N_3	875.	924.	1093.	768.	N_4	919.	955.	1105.	845.
C_1	773.	785.	765.	709.	C_2	906.	944.	1095.	830.

Table 18. Benchmark points for Model 17. See caption of Table 2 for details of notation.

work, we extended the survey to a particular extension of MSSM including right handed neutrinos. We chose the inverse seesaw model because of the possible large impact on the corrections to the Higgs mass. However with the usual boundary conditions prescribed for minimal gauge mediation it is hard to generate a large enhancement to the Higgs mass through the neutrino/sneutrino sector. In general gauge mediation framework, a large separate parameter for the sleptons should be prescribed such that these corrections become significant. Another way to increase the neutrino/sneutrino contributions would be to generate a large sneutrino mixing parameter through matter-messenger mixing. In the present work, we explored this possibility in great detail and surveyed all possible matter messenger mixing terms with leptonic doublet fields (L) and right handed neutrino fields (N^c). It turns out that in almost all the successful models, in addition to X_N, a significant correction to $M_{\tilde{L}}^2$ is also generated.

We classified all possible models by imposing lepton number on the messenger sector fields also. We found 17 such models. Both of the Type I (matter-messenger-messenger) and Type II (matter-matter-messenger). We analysed each model in detail by doing a full numerical analysis. The results are summarized in the Table 19.

We perform thorough numerical analysis by using SuSeFLAV considering $\tan\beta = 10$, $\mu_s = 10^{-4} \times m_e$ and $\Lambda = 100$ TeV (see Eq. (4.1)) for $x = 0.1$ and 0.5. The parameter x played an important role and the competition between one-loop and two-loop messenger-matter corrections is clear from the plots for these two values of x. In model 2, 3, 4, 5, 7, 11, 12, 13, 14, 15 and 17, there are two bands in λ, for $x = 0.5$. Except for the model 11 and 12, these bands get merged in to one for $x = 0.1$.

Model	Interaction	125 GeV Higgs		Range of λ	
Models with N^c					
		x=0.5	x=0.1	x=0.5	x=0.1
1.	$N^cQ\bar{Q}_m$	×	×	1.48	1.24
2.	$N^cU^c\bar{U}^c_m$	×	×	1.86	1.60
3.	$N^cD^c\bar{D}^c_m$	×	×	1.15	0.94
4.	$N^cLH^m_u$	✓	✓	1.84	1.61
5.	$N^cE^c\bar{E}^c_m$	×	×	2.10	1.60
6.	$N^cH_uH^m_d$	×	×	1.0	0.57
7.	$N^cH_dH^m_u$	✓	✓	1.68	1.52
8.	$\frac{1}{2}(N^c)^2S_m$	×	×	$\sqrt{4\pi}$	$\sqrt{4\pi}$
9.	N^cSS_m	×	×	$1.05-\sqrt{4\pi}$	$0.02-\sqrt{4\pi}$
10.	$N^cH^m_uH^m_d$	×	×	$\sqrt{4\pi}$	$\sqrt{4\pi}$
Models with L					
11.	$LQ\bar{D}^c_m$	✓	✓	1.21	1.09
12.	$LD^c\bar{Q}_m$	✓	✓	1.21	2.23
13.	$LE^cH^m_d$	✓	✓	1.20	0.93
14.	$LH_dE^c_m$	✓	✓	2.63	2.26
15.	LH_uS_m	✓	×	1.13	0.62
16.	LSH^m_u	✓	✓	$0.98-1.83$	$0.34-1.61$
17.	$LH^m_uS_m$	✓	✓	2.34	1.85

Table 19. Summary of all the models for both x=0.5 and x=0.1 case. The symbol ✓ shows that a 125 GeV Higgs can be achieved otherwise the symbol × is used. In the last two columns the range of the λ is shown. We mention the upper allowed value of λ and for the models where there is a lower bound we mention the allowed range (see model 9 and 16).

In the models 1, 2, 3, 5, 6, 8, 9, and 10, we do not get correct Higgs mass (see Table 19) because correction to $M^2_{\tilde{L}}$ is either zero or negative in the boundary. In the rest of the models, L directly couples to the messenger fields and thus in these model, $M^2_{\tilde{L}}$ gets both the positive two loop and negative one loop corrections at the boundary. For $x = 0.1$, two loop effect dominates over the one loop effect and $M^2_{\tilde{L}}$ becomes comparable to m_R. As a consequence, Higgs mass gets significant correction.

EWSB also played an important role in several models where H_u and H_d field are present in the messenger-matter Interaction. For example, in models 14, for $x = 0.5$, M_{H_u} gets both the negative and positive corrections whereas for $x = 0.1$ positive contributions dominate over the negative one-loop contribution. Thus with λ, this mass increases and EWSB can not be achieved beyond some value.

Models with messenger-matter corrections to $M_{\tilde{S}}$ are also interesting. The requirement

of non-tachyonic $M_{\tilde{S}}$ puts lower bound on value of λ. In model 16, for $x = 0.5$, complete parameter space is ruled out by this condition.

In the models where Q, U^c and H_u are interacting with the messenger field A_t term is generated at the boundary and these models are 1, 2, 6, 11 and 15. However, in models 1, 2 and 6 one cannot achieve a 125 GeV Higgs even for $x = 0.1$. Among all the 17 models, model 11 has benchmark points with the lightest $m_{\tilde{t}_1}$ mass. Thus this is the most promising model in the context of fine-tuning.

The set of models presented here has several unique features. The mass spectra is like the minimal gauge mediation models in the colored sector; the stops are light with small or negligible mixing. In the leptonic sector, the charged sleptons are light (typically except one eigenvalue), whereas the sneutrinos are heavy, close to the right handed neutrino mass scale. The typical collider signatures would mimic that of a minimal GMSB model, with large stau mixing, spectrum in LHC accessible range, and still have the lightest CP even higgs mass at 125 GeV.

Acknowledgement: We thank Biplob Bhattacherjee and Eung Jin Chun for discussions. SKV thanks CPHT, Ecole Polytechnique for hospitality during the final stages of this work. We thank Carlos E. M. Wagner for raising questions regarding factor of 1/2 in the Higgs mass calculation.

A One loop neutrino-sneutrino corrections to the Higgs mass

Tree level scalar potential (V_0) gets modified by one-loop Coleman-Weinberg potential ($\triangle V$)[69]. In principle one has to calculate vacuum by minimizing the complete potential i.e. $V_0 + \triangle V$; however in practice VEV of the Higgs fields are calculated by minimizing the tree level potential[1]. Thus the Higgs mass, which should be double derivative, contains some extra single derivative terms:

$$\Delta M_{ij}^2 = \frac{1}{2}\left(\frac{\partial^2 \Delta V}{\partial H_i \partial H_j} - \frac{\delta_{ij}}{H_i}\frac{\partial \Delta V}{\partial H_i}\right), \tag{A.1}$$

where $i, j = u, d$. Corrections from the top-stop sector are well-known. Here we are reviewing the correction to the Higgs mass from neutrino-sneutrino sector. Mass eigenvalues of these fields are already mentioned in § 3. Plugging these values into Coleman-Weinberg

[1]There is a conflict of factor of 1/2 in Eq. (A.1) between [49] and [51]. We resolve this issue and agree with [51]

potential, $\Delta M^2_{\nu ij}$ has to be calculated. We drop suffix ν from these terms for brevity.

$$\Delta M^2_{\rm uu} = \frac{1}{32\pi^2}\sum_{\alpha=1,2,3}\left(\tilde{L}_\alpha\,\tilde{B}^2_{\alpha u}+m^2_{\tilde{\nu}_\alpha}\left(\tilde{A}_{\alpha uu}-\frac{\tilde{B}_{\alpha u}}{H_u}\right)(\tilde{L}_\alpha-1)\right)\Bigg|_{H_u=\langle H_u\rangle} - \frac{1}{32\pi^2}\sum_{\alpha=1,2,3}\left(L_\alpha\,B^2_{\alpha u}+m^2_{\nu_\alpha}\left(A_{\alpha uu}-\frac{B_{\alpha u}}{H_u}\right)(L_\alpha-1)\right)\Bigg|_{H_u=\langle H_u\rangle}, \quad \text{(A.2)}$$

$$\Delta M^2_{\rm dd} = \frac{1}{32\pi^2}\sum_{\alpha=1,2,3}\left(\tilde{L}_\alpha\,\tilde{B}^2_{\alpha d}+m^2_{\tilde{\nu}_\alpha}\left(\tilde{A}_{\alpha dd}-\frac{\tilde{B}_{\alpha d}}{H_d}\right)(\tilde{L}_\alpha-1)\right)\Bigg|_{H_d=\langle H_d\rangle}, \quad \text{(A.3)}$$

$$\Delta M^2_{\rm ud} = \frac{1}{32\pi^2}\sum_{\alpha=1,2,3}\left(\tilde{L}_\alpha\,\tilde{B}_{\alpha u}\tilde{B}_{\alpha d}+m^2_{\tilde{\nu}_\alpha}\tilde{A}_{\alpha ud}(\tilde{L}_\alpha-1)\right)\Bigg|_{H_u=\langle H_u\rangle,H_d=\langle H_d\rangle}, \quad \text{(A.4)}$$

where

$$L_\alpha = \log\left(\frac{m^2_{\nu_\alpha}}{M^2_{\rm SUSY}}\right), \quad \tilde{L}_\alpha = \log\left(\frac{m^2_{\tilde{\nu}_\alpha}}{M^2_{\rm SUSY}}\right), \quad \text{(A.5)}$$

$$B_{\alpha j} = \frac{\partial m^2_{\nu_\alpha}}{\partial H_j}, \quad \tilde{B}_{\alpha j} = \frac{\partial m^2_{\tilde{\nu}_\alpha}}{\partial H_j}, \quad \text{(A.6)}$$

$$A_{\alpha jk} = \frac{\partial B_{\alpha j}}{\partial H_k}, \quad \tilde{A}_{\alpha jk} = \frac{\partial B_{\alpha j}}{\partial H_k}. \quad \text{(A.7)}$$

Explicit expressions for $\tilde{B}_{\alpha i}$ are as follows:

$$\tilde{B}_{1u} = \frac{2v_d\mu X_N y_N^2}{d_1}+2v_u\left(1+\frac{m_R^2}{d_2}+\frac{X_N^2}{d_1}\right)y_N^2, \quad \text{(A.8)}$$

$$\tilde{B}_{1d} = \frac{-2v_u\mu X_N y_N^2}{d_1}, \quad \text{(A.9)}$$

$$\tilde{B}_{2u} = \frac{-2v_d\mu X_N y_N^2}{d_1}+2v_u\left(1-\frac{X_N^2}{d_1}\right)y_N^2, \quad \text{(A.10)}$$

$$\tilde{B}_{2d} = \frac{2v_u\mu X_N y_N^2}{d_1}, \quad \text{(A.11)}$$

$$\tilde{B}_{3u} = \frac{-2v_u m_R^2 y_N^2}{d_2}, \quad \text{(A.12)}$$

$$\tilde{B}_{3d} = 0. \quad \text{(A.13)}$$

Similarly one can calculate the $\tilde{A}_{\alpha ij}$ terms:

$$\tilde{A}_{1uu} = \frac{2v_d^2\mu^2 y_N^2}{v_u^2 d_1} + \frac{4v_d\mu X_N y_N^2}{v_u d_1} + 2\left(1 + \frac{m_R^2}{d_2} + \frac{X_N^2}{d_1}\right) y_N^2, \tag{A.14}$$

$$\tilde{A}_{1ud} = \frac{-2v_d\mu^2 y_N^2}{v_u d_1} - \frac{2\mu X_N y_N^2}{d_1}, \tag{A.15}$$

$$\tilde{A}_{1dd} = \frac{2\mu^2 y_N^2}{d_1}, \tag{A.16}$$

$$\tilde{A}_{2uu} = \frac{-2v_d^2\mu^2 y_N^2}{v_u^2 d_1} - \frac{4v_d\mu X_N y_N^2}{v_u d_1} + 2\left(1 - \frac{X_N^2}{d_1}\right) y_N^2, \tag{A.17}$$

$$\tilde{A}_{2ud} = \frac{2v_d\mu^2 y_N^2}{v_u d_1} + \frac{2\mu X_N y_N^2}{d_1}, \tag{A.18}$$

$$\tilde{A}_{2dd} = \frac{-2\mu^2 y_N^2}{d_1}, \tag{A.19}$$

$$\tilde{A}_{3uu} = \frac{-2m_R^2 y_N^2}{d_2}, \tag{A.20}$$

$$\tilde{A}_{3ud} = 0, \tag{A.21}$$

$$\tilde{A}_{3dd} = 0. \tag{A.22}$$

Similarly $B_{\alpha i}$ terms are:

$$B_{1u} = \frac{4v_u^3 y_N^4 \mu_S^2}{m_R^4}, \tag{A.23}$$

$$B_{2u} = \frac{2v_u y_N^2 \left(\frac{v_u^2 y_N^2}{2m_R} + m_R\right)}{m_R}, \tag{A.24}$$

$$B_{3u} = \frac{2v_u y_N^2 \left(\frac{v_u^2 y_N^2}{2m_R} + m_R\right)}{m_R}, \tag{A.25}$$

$$B_{1d} = 0, \tag{A.26}$$

$$B_{2d} = 0, \tag{A.27}$$

$$B_{3d} = 0. \tag{A.28}$$

Finally the $A_{\alpha ij}$ terms are as follows:

$$A_{1uu} = \frac{12 v_u^2 y_N^4 \mu_S^2}{m_R^4}, \tag{A.29}$$

$$A_{2uu} = \frac{2 v_u^2 y_N^4}{m_R^2} + \frac{2 y_N^2 \left(\frac{v_u^2 y_N^2}{2 m_R} + m_R\right)}{m_R}, \tag{A.30}$$

$$A_{3uu} = \frac{2 v_u^2 y_N^4}{m_R^2} + \frac{2 \left(\frac{v_u^2 y_N^2}{2 m_R} + m_R\right) y_N^2}{m_R}, \tag{A.31}$$

$$A_{1ud} = 0, \tag{A.32}$$

$$A_{2ud} = 0, \tag{A.33}$$

$$A_{3ud} = 0, \tag{A.34}$$

$$A_{1dd} = 0, \tag{A.35}$$

$$A_{2dd} = 0, \tag{A.36}$$

$$A_{3dd} = 0. \tag{A.37}$$

Now being equipped with the above formulas one can calculate Higgs mass. We are here giving a simple formula for alignment limit:

$$m_h^2 = m_Z^2 \cos^2 2\beta + \text{ top-stop correction } + \sin^2\beta \triangle M_{uu}^2 + \sin 2\beta \triangle M_{ud}^2 + \cos^2\beta \triangle M_{dd}^2. \tag{A.38}$$

References

[1] P. Byakti and T. S. Ray, *Burgeoning the Higgs mass to 125 GeV through messenger-matter interactions in GMSB models*, *JHEP* **05** (2013) 055, [1301.7605].

[2] J. A. Evans and D. Shih, *Surveying Extended GMSB Models with m_h=125 GeV*, *JHEP* **08** (2013) 093, [1303.0228].

[3] A. Salam and J. A. Strathdee, *Supergauge Transformations*, *Nucl. Phys.* **B76** (1974) 477–482.

[4] P. Fayet and S. Ferrara, *Supersymmetry*, *Phys. Rept.* **32** (1977) 249–334.

[5] H. P. Nilles, *Supersymmetry, Supergravity and Particle Physics*, *Phys. Rept.* **110** (1984) 1–162.

[6] J. Wess and J. Bagger, *Supersymmetry and supergravity*. 1992.

[7] S. P. Martin, *A Supersymmetry primer*, hep-ph/9709356.

[8] P. Fayet, *Supersymmetry and Weak, Electromagnetic and Strong Interactions*, *Phys. Lett.* **B64** (1976) 159.

[9] S. K. Vempati, *Introduction to MSSM*, 1201.0334.

[10] G. F. Giudice and R. Rattazzi, *Theories with gauge mediated supersymmetry breaking*, *Phys. Rept.* **322** (1999) 419–499, [hep-ph/9801271].

[11] ATLAS collaboration, G. Aad et al., *Observation of a new particle in the search for the Standard Model Higgs boson with the ATLAS detector at the LHC*, *Phys. Lett.* **B716** (2012) 1–29, [1207.7214].

[12] CMS collaboration, S. Chatrchyan et al., *Observation of a new boson at a mass of 125 GeV with the CMS experiment at the LHC*, *Phys. Lett.* **B716** (2012) 30–61, [1207.7235].

[13] P. Draper, P. Meade, M. Reece and D. Shih, *Implications of a 125 GeV Higgs for the MSSM and Low-Scale SUSY Breaking*, *Phys. Rev.* **D85** (2012) 095007, [1112.3068].

[14] K. Intriligator and M. Sudano, *General Gauge Mediation with Gauge Messengers*, *JHEP* **06** (2010) 047, [1001.5443].

[15] P. Grajek, A. Mariotti and D. Redigolo, *Phenomenology of General Gauge Mediation in light of a 125 GeV Higgs*, *JHEP* **07** (2013) 109, [1303.0870].

[16] Z. Kang, T. Li, T. Liu, C. Tong and J. M. Yang, *A Heavy SM-like Higgs and a Light Stop from Yukawa-Deflected Gauge Mediation*, *Phys. Rev.* **D86** (2012) 095020, [1203.2336].

[17] A. Albaid and K. S. Babu, *Higgs boson of mass 125 GeV in GMSB models with messenger-matter mixing*, *Phys. Rev.* **D88** (2013) 055007, [1207.1014].

[18] T. Han and R.-J. Zhang, *Direct messenger - matter interactions in gauge - mediated supersymmetry breaking models*, *Phys. Lett.* **B428** (1998) 120–128, [hep-ph/9802422].

[19] N. Craig, S. Knapen, D. Shih and Y. Zhao, *A Complete Model of Low-Scale Gauge Mediation*, *JHEP* **03** (2013) 154, [1206.4086].

[20] J. L. Evans, M. Ibe and T. T. Yanagida, *Relatively Heavy Higgs Boson in More Generic Gauge Mediation*, *Phys. Lett.* **B705** (2011) 342–348, [1107.3006].

[21] S. P. Martin and J. D. Wells, *Implications of gauge-mediated supersymmetry breaking with vector-like quarks and a 125 GeV Higgs boson*, *Phys. Rev.* **D86** (2012) 035017, [1206.2956].

[22] J. A. Casas, J. M. Moreno, S. Robles and K. Rolbiecki, *Reducing the Fine-Tuning of Gauge-Mediated SUSY Breaking*, 1602.06892.

[23] R. Ding, T. Li, L. Wang and B. Zhu, *Towards the Natural Gauge Mediation*, *JHEP* **10** (2015) 154, [1506.00359].

[24] A. Delgado, M. Garcia-Pepin and M. Quiros, *GMSB with Light Stops*, *JHEP* **08** (2015) 159, [1505.07469].

[25] T. Jeliski, *$SO(10)$ inspired extended GMSB models*, *PoS* **CORFU2014** (2015) 089, [1505.06722].

[26] J. A. Evans, D. Shih and A. Thalapillil, *Chiral Flavor Violation from Extended Gauge Mediation*, *JHEP* **07** (2015) 040, [1504.00930].

[27] M. Backovi, A. Mariotti and M. Spannowsky, *Signs of Tops from Highly Mixed Stops*, *JHEP* **06** (2015) 122, [1504.00927].

[28] A. Basirnia, D. Egana-Ugrinovic, S. Knapen and D. Shih, *125 GeV Higgs from Tree-Level A-terms*, *JHEP* **06** (2015) 144, [1501.00997].

[29] W. Fischler and W. Tangarife, *Vector-like Fields, Messenger Mixing and the Higgs mass in Gauge Mediation*, *JHEP* **05** (2014) 151, [1310.6369].

[30] T. Jeliski, *On messengers couplings in extended GMSB models*, *JHEP* **09** (2013) 107, [1305.6277].

[31] L. Calibbi, P. Paradisi and R. Ziegler, *Gauge Mediation beyond Minimal Flavor Violation*, *JHEP* **06** (2013) 052, [1304.1453].

[32] V. S. Mummidi and S. K. Vempati, *A little more Gauge Mediation and the light Higgs mass*, *Nucl. Phys.* **B881** (2014) 181–205, [1311.4280].

[33] K. S. Babu, I. Gogoladze, M. U. Rehman and Q. Shafi, *Higgs Boson Mass, Sparticle Spectrum and Little Hierarchy Problem in Extended MSSM*, *Phys. Rev.* **D78** (2008) 055017, [0807.3055].

[34] M. Endo, K. Hamaguchi, S. Iwamoto and N. Yokozaki, *Higgs Mass and Muon Anomalous Magnetic Moment in Supersymmetric Models with Vector-Like Matters*, *Phys. Rev.* **D84** (2011) 075017, [1108.3071].

[35] M. Endo, K. Hamaguchi, S. Iwamoto and N. Yokozaki, *Higgs mass, muon g-2, and LHC prospects in gauge mediation models with vector-like matters*, *Phys. Rev.* **D85** (2012) 095012, [1112.5653].

[36] K. Nakayama and N. Yokozaki, *Peccei-Quinn extended gauge-mediation model with vector-like matter*, *JHEP* **11** (2012) 158, [1204.5420].

[37] M. Asano, Y. Nakai and N. Yokozaki, *A New Scheme for NMSSM in Gauge Mediation*, *JHEP* **01** (2016) 066, [1510.08033].

[38] G. Mittag, *Search for a Light NMSSM Higgs Boson in the b-Quark Final State at the LHC*. PhD thesis, U. Hamburg, Dept. Phys., Hamburg, 2015.

[39] K. Kowalska, J. Paweczyk and E. M. Sessolo, *Flavored gauge mediation in the Peccei-Quinn NMSSM*, *JHEP* **12** (2015) 148, [1508.04142].

[40] F. Domingo, *A New Tool for the study of the CP-violating NMSSM*, *JHEP* **06** (2015) 052, [1503.07087].

[41] M. Cahill-Rowley, J. Gainer, J. Hewett and T. Rizzo, *Towards a Supersymmetric Description of the Fermi Galactic Center Excess*, *JHEP* **02** (2015) 057, [1409.1573].

[42] U. Ellwanger and A. M. Teixeira, *NMSSM with a singlino LSP: possible challenges for searches for supersymmetry at the LHC*, *JHEP* **10** (2014) 113, [1406.7221].

[43] P. Athron, J.-h. Park, D. Stckinger and A. Voigt, *FlexibleSUSYA spectrum generator generator for supersymmetric models*, *Comput. Phys. Commun.* **190** (2015) 139–172, [1406.2319].

[44] B. C. Allanach, P. Athron, L. C. Tunstall, A. Voigt and A. G. Williams, *Next-to-Minimal SOFTSUSY*, *Comput. Phys. Commun.* **185** (2014) 2322–2339, [1311.7659].

[45] T. T. Yanagida, N. Yokozaki and K. Yonekura, *Higgs Boson Mass in Low Scale Gauge Mediation Models*, *JHEP* **10** (2012) 017, [1206.6589].

[46] A. de La Puente and W. Tangarife, *A Singlet Extension of the MSSM with a Dark Matter Portal*, *JHEP* **07** (2014) 087, [1309.6359].

[47] M. E. Krauss, W. Porod and F. Staub, *SO(10) inspired gauge-mediated supersymmetry breaking*, *Phys. Rev.* **D88** (2013) 015014, [1304.0769].

[48] A. M. Iyer, V. S. Mummidi and S. K. Vempati, *Gravitational rescue of minimal gauge mediation*, *Int. J. Mod. Phys.* **A31** (2016) 1650045, [1408.4462].

[49] A. Elsayed, S. Khalil and S. Moretti, *Higgs Mass Corrections in the SUSY B-L Model with Inverse Seesaw*, *Phys. Lett.* **B715** (2012) 208–213, [1106.2130].

[50] P. Draper and H. E. Haber, *Decoupling of the Right-handed Neutrino Contribution to the Higgs Mass in Supersymmetric Models*, *Eur. Phys. J.* **C73** (2013) 2522, [1304.6103].

[51] J. Guo, Z. Kang, T. Li and Y. Liu, *Higgs boson mass and complex sneutrino dark matter in the supersymmetric inverse seesaw models*, *JHEP* **02** (2014) 080, [1311.3497].

[52] E. J. Chun, V. S. Mummidi and S. K. Vempati, *Anatomy of Higgs mass in Supersymmetric Inverse Seesaw Models*, *Phys. Lett.* **B736** (2014) 470–477, [1405.5478].

[53] L. Calibbi, L. Ferretti, A. Romanino and R. Ziegler, *Gauge coupling unification, the GUT scale, and magic fields*, *Phys. Lett.* **B672** (2009) 152–157, [0812.0342].

[54] P. Byakti and D. Ghosh, *Magic Messengers in Gauge Mediation and signal for 125 GeV boosted Higgs boson*, *Phys. Rev.* **D86** (2012) 095027, [1204.0415].

[55] P. Meade, N. Seiberg and D. Shih, *General Gauge Mediation*, *Prog. Theor. Phys. Suppl.* **177** (2009) 143–158, [0801.3278].

[56] T. T. Dumitrescu, Z. Komargodski, N. Seiberg and D. Shih, *General Messenger Gauge Mediation*, *JHEP* **05** (2010) 096, [1003.2661].

[57] M. Dine, Y. Nir and Y. Shirman, *Variations on minimal gauge mediated supersymmetry breaking*, *Phys. Rev.* **D55** (1997) 1501–1508, [hep-ph/9607397].

[58] G. R. Dvali, G. F. Giudice and A. Pomarol, *The Mu problem in theories with gauge mediated supersymmetry breaking*, *Nucl. Phys.* **B478** (1996) 31–45, [hep-ph/9603238].

[59] A. Delgado, G. F. Giudice and P. Slavich, *Dynamical mu term in gauge mediation*, *Phys. Lett.* **B653** (2007) 424–433, [0706.3873].

[60] Z. Komargodski and N. Seiberg, *mu and General Gauge Mediation*, *JHEP* **03** (2009) 072, [0812.3900].

[61] Z. Chacko and E. Ponton, *Yukawa deflected gauge mediation*, *Phys. Rev.* **D66** (2002) 095004, [hep-ph/0112190].

[62] G. F. Giudice and R. Rattazzi, *Extracting supersymmetry breaking effects from wave function renormalization*, *Nucl. Phys.* **B511** (1998) 25–44, [hep-ph/9706540].

[63] A. Mariotti, M. Backovic and M. Spannowsky, *Signs of Tops from Highly Mixed Stops*, *PoS* **PLANCK2015** (2015) 080.

[64] L. Calibbi, P. Paradisi and R. Ziegler, *Lepton Flavor Violation in Flavored Gauge Mediation*, *Eur. Phys. J.* **C74** (2014) 3211, [1408.0754].

[65] R. N. Mohapatra and P. B. Pal, *Massive neutrinos in physics and astrophysics. Second edition*, *World Sci. Lect. Notes Phys.* **60** (1998) 1–397.

[66] R. N. Mohapatra and J. W. F. Valle, *Neutrino Mass and Baryon Number Nonconservation in Superstring Models*, *Phys. Rev.* **D34** (1986) 1642.

[67] I. Gogoladze, B. He and Q. Shafi, *Inverse Seesaw in NMSSM and 126 GeV Higgs Boson*, *Phys. Lett.* **B718** (2013) 1008–1013, [1209.5984].

[68] F. del Aguila, J. de Blas and M. Perez-Victoria, *Effects of new leptons in Electroweak Precision Data*, *Phys. Rev.* **D78** (2008) 013010, [0803.4008].

[69] S. R. Coleman and E. J. Weinberg, *Radiative Corrections as the Origin of Spontaneous Symmetry Breaking*, *Phys. Rev.* **D7** (1973) 1888–1910.

[70] CMS collaboration, V. Khachatryan et al., *Search for supersymmetry in events with photons and missing transverse energy in pp collisions at 13 TeV*, *Submitted to: Phys. Lett. B* (2016) , [1611.06604].

[71] ATLAS collaboration, G. Aad et al., *Search for photonic signatures of gauge-mediated supersymmetry in 8 TeV pp collisions with the ATLAS detector*, *Phys. Rev.* **D92** (2015) 072001, [1507.05493].

[72] M. Viel, J. Lesgourgues, M. G. Haehnelt, S. Matarrese and A. Riotto, *Constraining warm dark matter candidates including sterile neutrinos and light gravitinos with WMAP and the Lyman-alpha forest*, *Phys. Rev.* **D71** (2005) 063534, [astro-ph/0501562].

[73] M. Kawasaki, F. Takahashi and T. T. Yanagida, *Gravitino overproduction in inflaton decay*, *Phys. Lett.* **B638** (2006) 8–12, [hep-ph/0603265].

[74] D. Chowdhury, R. Garani and S. K. Vempati, *SuSeFLAV: A Program for calculating supersymmetric spectra and lepton flavor violation*, *Pramana* **79** (2012) 887–889, [1112.4403].